

Increased sexual dimorphism evolves in a fossil stickleback following ecological release from fish piscivores

Matthew Stuart^{1,2}, Allison Ozark³, Raheyima Siddiqui³, Akhil Ghosh^{1,2},
Samantha Swank³, Michael A. Bell⁴, Gregory J. Matthews^{1,2}, and Yoel E. Stuart^{3,+}

¹ Department of Mathematics and Statistics, Loyola University Chicago, Chicago, IL, U

² Center for Data Science and Consulting, Loyola University Chicago, Chicago, IL, U

³ Department of Biology, Loyola University Chicago, Chicago, IL, USA

⁴ University of California Museum of Paleontology, Berkeley, CA, USA

⁺ Corresponding: ystuart@luc.edu

Abstract

Everyone loves the stickle

Keywords: Stickle

1 Introduction

Ecological release theory suggests that a population’s niche should change when important species interactions like resource competition or predation are relaxed or removed (reviewed in Herrmann, Stroud, and Losos (2021)). Removal is posited to create ecological opportunity—i.e., aspects of the niche become newly accessible, and the focal population shifts and/or expands its resource use new resources (Parent and Crespi (2009); Herrmann, Stroud, and Losos (2021)). Ecological release may then be followed by adaptive morphological evolution as traits change to reflect the new niche (Parent and Crespi (2009); Herrmann, Stroud, and Losos (2021)).

For example, a population undergoing ecological release can experience disruptive selection on males and females stemming from intraspecific competition over newly accessible resources (Bolnick and Doebeli (2003); Bolnick and Lau (2008); Cooper, Gilman, and Boughman (2011)). This is predicted to result in intersexual divergence in habitat use and associated phenotypes (Schoener (1968); Shine (1989); Bolnick and Doebeli (2003); Butler and Losos (2007); Bolnick and Lau (2008); Cooper, Gilman, and Boughman (2011); but see Stuart et al. (2021); Blain (2022)). Such competition-driven “intraspecific character displacement” between the sexes is therefore one explanation for the evolution of sexual dimorphism (Pfennig and Pfennig (2012); De Lisle and Rowe (2015); De Lisle and Rowe (2017), De Lisle, Paiva, and Rowe (2018)).

Much of the theory and empirical data for character displacement between the sexes is based on release from resource competition specifically (e.g., Bolnick and Doebeli (2003); Cooper, Gilman, and Boughman (2011); Pfennig and Pfennig (2012); De Lisle and Rowe (2015); De Lisle, Paiva, and Rowe (2018)). However, release from predation might also drive the evolution of increased sexual dimorphism because an absence of predators should generate ecological opportunity (Reimchen and Nosil (2004); Parent and Crespi (2009); Herrmann, Stroud, and Losos (2021)).

Here, we tested the prediction that a release from predation results in the evolution of increased sexual dimorphism using a well-preserved, finely-resolved sequence of a fossil three-spine stickleback fish (*Gasterosteus doryssus*). The sequence in this depositional environment is comprised of two lineages (Bell (2009); Cerasoni, Bell, and Stuart (2024)). Lineage I was a low-armor form with zero to one dorsal spines and highly reduced pelvises, on average. Lineage I lasted for at least 93,000 years before it was replaced by a second lineage, suddenly, likely on the order of years (Bell, Baumgartner, and Osion (1985); Stuart et al. unpublished data). Lineage II appeared in the depositional environment fully armored, with complete pelvic girdles, two pelvic spines, and three dorsal spines (Bell, Travis, and Blouw (2006); Stuart, Travis, and Bell (2020)). It then immediately began evolving adaptive reduction in its armor traits (Hunt, Bell, and Travis (2008); Stuart, Travis, and Bell (2020)) until it

reached the same low-armor state previously held by lineage I.

The observation of 93,000 years of low-armor stasis in lineage I (Bell, Baumgartner, and Oslen (1985)) and the observation of rapid evolution of armor loss by lineage II, both suggest that this depositional environment lacked piscivorous fish like trout and other salmonids known to prey on modern threespine stickleback. Armor presence in extant threespine stickleback (*Gasterosteus aculeatus*) correlates strongly with the presence of vertebrate piscivores; populations with less predation pressure typically have less armor (Reimchen (1994), Reimchen and Nosil (2004); Bell et al. (1993); Roesti et al. (2023)). In our paleolake basin, only three fossil trout have been found in the same section of rock that has revealed >20,000 threespine stickleback fossils as well as occasional killifish (*Fundulus nevadensis*) (Bell (2009); Cerasoni, Bell, and Stuart (2024)). Thus, we reconstruct an evolutionary history in which it is likely that lineage II migrated from a nearby paleolake basin that had predators since it was armored when it arrived (Bell (2009); Cerasoni, Bell, and Stuart (2024)). Lineage II then experienced release from predators in the focal paleolake basin, generating the initial conditions of evolutionary models predicting the evolution of increased sexual dimorphism following ecological release. We test this prediction here.

A major challenge in the study of fossilized sexual dimorphism is assigning sex to individual specimens in the first place (Hone and Mallon (2017); Mallon (2017); Saitta et al. (2020)). This typically cannot be done directly, except for taxa whose sexes are distinguished by the presence or absence of sex-specific characters that preserve well. Instead, paleobiologists often resort to statistical detection of sex and sexual dimorphism, including tests for normality and bimodality in trait distributions (e.g., Mallon (2017)), mixture modeling (e.g., Mallon (2017)), divergence in growth curves (e.g., Saitta et al. (2020)), and emphasis on effect size statistics rather than significance testing (e.g., Saitta et al. (2020)). However, dimorphic signal can be masked by noise introduced by factors both biological and artifactual, including extended growth during ontogeny, age-based bias in survivorship, small sample sizes, time averaging, and taphonomic bias (Godfrey, Lyon, and Sutherland (1993); Koscinski and Pietraszewski (2004); Hone and Mallon (2017); reviewed in Mallon (2017); reviewed in Saitta et al. (2020)). Thus, the best approach to sex classification is likely one of total evidence (Saitta et al. (2020)), including comparison to closely-related, extant species of known sex (e.g., Hone and Mallon (2017); Saitta et al. (2020)).

For our study, we inferred sex in *G. doryssus* fossils by comparing multivariate morphological trait data from lineage II samples to the same multivariate trait set collected from multiple populations in the closely-related, extant Threespine Stickleback species complex (*Gasterosteus aculeatus*). Crucially, we determined *G. aculeatus* sex directly via dissection and/or PCR genotyping. This enabled us to use Multiple Imputation by Chained Equations (MICE; Buuren and Groothuis-Oudshoorn (2011)) to build a predictive multiple imputation algorithm (Little and Rubin (2002)) based on the multivariate morphology of *G. aculeatus*

individuals of known sex. We applied this algorithm to the fossil data to impute individual sex based on morphology, treating fossil sex as a missing variable. With sex assigned to fossil specimens, we fit a modified Ornstein-Uhlenbeck (OU) (Uhlenbeck and Ornstein (1930)) model using a Bayesian framework that accounts for uncertainty in sex classification to test for evolution of sexual dimorphism in each trait over ~16,000 years of lineage II.

2 Data

2.1 Fossil Specimen Data

We used *Gasterosteus doryssus* data that were previously reported by Stuart, Travis, and Bell (2020), Voje, Bell, and Stuart (2022), and Siddiqui et al. (2024). Briefly, the data were collected from fossil Series K from Quarry D (Cerasoni, Bell, and Stuart (2024)), dug from an open pit diatomite mine at 9.526° N, 119.094° W, near Hazen, Nevada, USA. Series K consisted of 18 samples taken at ~1000-year intervals, and mean sample times span ~16,363 years. Fish from series K were measured for 16 ecomorphological traits related to armor, swimming, and feeding (Table 1). Series K started at the previously documented horizon when lineage I was replaced by lineage II. The tempo and mode of lineage II armor reduction during this sequence suggests adaptive evolution by natural selection (Hunt, Bell, and Travis (2008)), and we focus on the multivariate evolution of sexual dimorphism by this second lineage.

The lineage II fossil data consist of 814 specimens of unknown sex sampled across the 18 K series samples. Figure 1 shows the sample size for each of the 18 samples. There are at least 22 specimens in each sample with a high of 67 specimens in sample 7.

Trait Name	Trait	
	Code	Trait Description
Standard Length	stl	Distance from anterior tip of premaxilla to posterior end of last vertebra (hypural plate)
Dorsal Spine	mds	Number of dorsal spines from 0 to 3
Dorsal Fin Ray	mdf	Number of bones in the dorsal fin posterior to the third dorsal spine (i.e., soft dorsal fin rays)
Anal Fin Ray	maf	Number of bones in the anal fin posterior to the anal spine (i.e., soft dorsal fin rays)
Abdominal Vertebra	mav	Number of vertebrae anterior to the first vertebra contacting an anal fin pterygiophore (Aguirre et al. 2014)

Trait Name	Trait Code	Trait Description
Caudal Vertebra	mcv	Number of vertebrae posterior to and including the first vertebra contacting an anal fin pterygiophore (Aguirre et al. 2014)
Pterygiophore number	mpt	Number of pterygiophores anterior to but excluding the pterygiophore under the third dorsal spine, which is immediately anterior to and contiguous with the dorsal fin
Pelvic Spine length	lps.sc	Length from the base of one pelvic spine above its articulation with the pelvic girdle to its distal tip
Ectocoracoid	ect.sc	Length between the anterior and posterior tips of the shoulder girdle base (i.e., ectocoracoid)
Pelvic Girdle	tpg.sc	Length between the anterior to posterior tips along midline. If vestigial, the sum of longest anterior-posterior axis for the vestiges
Cleithrum length	cle.sc	Length from free dorsal tip to ventral tip of the cleithrum on the anterior margin of the shoulder girdle (i.e., cleithrum)
Premaxilla	pmx.sc	Length from the anterior tip of the premaxilla to the distal tip of the ascending process of the premaxilla
Dorsal Spine	Ds#.sc	Length from the base of a dorsal spine above the pterygiophore to its distal tip along the anterior edge
Pterygiophore	lpt.sc	Distance between the anterior to posterior tips of the pterygiophore immediately preceding the 3rd dorsal spine (when present)

This table caption should be part of the table. Top row.. -YS Table: Traits and trait descriptions. ‘sc’ denotes size correction of trait against standard length. Names of bones follow Bowne (1994) unless otherwise noted.

2.2 Extant Specimen data

To span the gamut of stickleback diversity for our predictive imputation model, we sampled modern stickleback from lakes containing generalist stickleback populations (Hendry et al. (2009); Bolnick (2011)) and from lakes containing benthic-limnetic species pairs (Baumgartner, Bell, and Weinberg (1988); Schluter and McPhail (1992)). The generalist specimens used here were collected by YES in 2013 and were previously described in Stuart et al. (2017) (Table S1). These samples were fixed in formalin, then stained for bone with Alizarin Red in 2013. Benthic and limnetic specimens were kindly loaned by D. Schluter and S. Blain at the University of British Columbia. The Schluter lab collected benthic and limnetic

individuals from Enos Lake in 1988 and from Emily Lake, Little Quarry Lake, Paxton Lake, and Priest Lake in 2018 (Table S1). The Enos specimens had been fixed whole in formalin and stored in 40% isopropanol. The specimens from the other lakes were initially preserved whole in 95% ethanol in the field before being gradually transferred to water then formalin in the lab and ultimately stored in 40% isopropanol. In 2019, we stained these specimens for bone using Alizarin Red. We next replicated fossil data collection (Table 1) on these extant specimens. Standard length as well as pelvic-spine length on each side were measured with calipers. We used a dissection microscope to count dorsal spines, pelvic spines, dorsal-fin rays, and anal-fin rays. Right and left-side pelvic girdle lengths and ectocoracoid lengths were measured from ventral photographs taken using a Canon EOS Rebel T7 with a Tamron 16-300 mm MACRO lens mounted on a leveled Kaiser RS1 copy stand. Specimens were held in place for ventral photographs using a small tabletop vise with an attached scale bar. Lateral X-rays were used to measure dorsal spine length, number of pterygiophores anterior to the pterygiophore holding the third spine, length of the pterygiophore just anterior to the third spine, cleithrum length, and pre-maxilla ascending branch length. We also counted vertebrae from the X-rays: abdominal vertebrae were counted anterior to the first vertebra with a haemal spine contacting an anal fin pterygiophore. Caudal vertebrae were posterior, including the first vertebra with the haemal spine contacting the anal fin pterygiophore (following Aguirre, Walker, and Gideon (2014)). X-rays were taken with an AXR Hot Shot X-ray Machine (Associated X-ray Corporation) at the Field Museum of Natural History. Specimens were exposed at 35kV and 4mA. Small fish were exposed for 7s, medium fish for 8s, and large fish for 10s. We developed the film and scanned individual images of each fish using the B&W Negatives setting on an Epson Perfection 4990 Photo flatbed at 2400 dpi. Measurements from photographs and X-rays were taken with FIJI (Schindelin et al. (2012)) and its plugin ObjectJ (<https://sils.fnwi.uva.nl/bcb/objectj/>).

We dissected individuals from the generalist populations (Table S1) to determine sex from the gonads. Individuals from the species-pair lakes (Table S1) were previously sexed by the Schluter lab, using either dissection or a genotyping protocol (Whom, personal communication).

The extant data used here consists of a total of 367 specimens all with known sex (Table S1). Of these, there are 202 and 165 female and male specimens, respectively.

2.3 Outlier analysis and size correction.

To check for outliers, we calculated within-group means and standard deviations for each trait separately for K series fossil specimens (pooled across samples) and for extant specimens (within generalist, benthic, or limnetic categories). We noted trait values greater than 3.0 standard deviations from the mean as potential outliers. We deemed 3.0 s.d. to be a

reasonable threshold for detecting errors without excluding biologically relevant values. We checked whether these potential outliers were a result of data entry and collection error and corrected them if they were. We turned the remaining outlier trait values to NAs. We size-corrected continuous traits only, as they varied with size, unlike count traits that are fixed during early development. We regressed each trait on standard length using a mixed-model regression, pooling all specimens, following Stuart et al. (2017). We appended the size corrected data to the uncorrected trait data frame and used all of our data (raw and size-corrected) to build the imputation model described next.

2.4 Missing data imputation, including fossil sex

Briefly, We used multiple imputation (Little and Rubin (2002)) to impute the sex of the fossils. Let \mathbf{W} be an $(n_{\text{extant}} + n_{\text{fossil}}) \times 1$ vector of the covariate sex of the stickleback fish and \mathbf{Y} be an $(n_{\text{extant}} + n_{\text{fossil}}) \times K$ matrix of the K phenotypes of interest. Because the sex of the fossilized stickleback fish is unobservable, we further define $\mathbf{W} = (\mathbf{W}_{\text{extant}}^T, \mathbf{W}_{\text{fossil}}^T)^T$ where $\mathbf{W}_{\text{extant}}$ and $\mathbf{W}_{\text{fossil}}$ are the $n_{\text{extant}} \times 1$ and $n_{\text{fossil}} \times 1$ vectors of the observed extant sex and missing fossil sex, respectively. We imputed missing sex for the fossil data by sampling from the posterior predictive distribution $P(\mathbf{W}_{\text{fossil}} | \mathbf{W}_{\text{extant}}, \mathbf{Y})$ using the multiple imputation by chained equations (MICE) algorithm (Buuren and Groothuis-Oudshoorn (2011)) with predictive mean matching, implemented in R (CITATION). Traditionally, the choice for the number of completed data sets is a relatively small number such as $M = 5$ or $M = 10$. However, Zhou and Reiter (2010) recommend a larger number of imputed data sets if users intend on performing Bayesian analysis after imputation. Therefore, we imputed $M = 100$ complete datasets.

presumably this also imputes missing data in the other traits? We should probably say that explicitly. -YS AKHIL'S METHODS FOR VALIDATION OF THE IMPUTATION MODEL GOES HERE THE POOLING DESCRIBED IN THE NEXT SENTENCE. WAS IT DONE, AND IF SO, HOW WAS IT USED IN DOWNSTREAM ANALYSES. MATT SAYS THAT HE RAN IS MODELS ON EACH IMPUTED DATA SET. -YS We then pooled all of the draws from the posterior distribution across all the imputed data sets to estimate the posterior distributions of our parameters of interest (i.e., the trait values), rather than using Rubin's combining rules, following Zhou and Reiter (2010). We used these posterior distributions in our Bayesian analysis.

2.5 Modeling trait means through time for males and females

The goal of our analysis was to estimate fossil trait means through time, by sex, while incorporating uncertainty in the imputed data, especially uncertainty sex classification. We

took a Bayesian approach because imputation is the process of sampling from a posterior predictive distribution of missing data, given observed data. **THIS NEEDS MORE WORK TO JUSTIFY THE BAYESIAN APPROACH. -YS**

DOES THE NEXT SENTENCE CONTRADICT THE PREVIOUS ONE? BELOW, WE SAY THAT WE USED EACH IMPUTED DATA SET. ABOVE, WE SAY THAT WE POOLED ACROSS IMPUTED DATA SETS.-YS To estimate fossil sample means through time, we first dropped the extant individuals from our imputed data sets. Then, for a given imputed dataset, we let W_{ij} be the imputed sex and \mathbf{Y}_{ij} be the $K \times 1$ vector of phenotypes for stickleback fossil j at time t_i where $i = 1, \dots, T$ and $j = 1, \dots, n_t$. In addition, we denote $Y_{K,ij}$, the last variable in \mathbf{Y}_{ij} , to be the standard length of each fish individual, a measure of body size.

$$Y_{K,ij} \stackrel{iid}{\sim} \begin{cases} \mathcal{N}(\mu_{K,ft_i}, \sigma_K^2), & W_{ij} = \text{Female} \\ \mathcal{N}(\mu_{K,mt_i}, \sigma_K^2), & W_{ij} = \text{Male} \end{cases} . \quad (1)$$

It is reasonable to assume that the other continuous traits will have some correlation with standard length (**CITATION**). We account for this by adding an additional parameter, γ_k , If $Y_{k,ij}$ is a continuous trait, then

$$Y_{k,ij} \stackrel{iid}{\sim} \begin{cases} \mathcal{N}(\mu_{k,ft_i} + \gamma_k Y_{K,ij}, \sigma_k^2), & W_{ij} = \text{Female} \\ \mathcal{N}(\mu_{k,mt_i} + \gamma_k Y_{K,ij}, \sigma_k^2), & W_{ij} = \text{Male} \end{cases} . \quad (2)$$

If $Y_{k,ij}$ is a discrete trait, the conventional modelling method is to fit a Poisson distribution. However, because the empirical fossil data violate the assumption that the Poisson variance is equal to its mean, we fit discrete traits to a generalized Poisson model as defined in (**GeneralizedPoisson?**). Specifically, if $X \sim GP(\lambda, \alpha)$, then

$$P(X = x) = \begin{cases} \frac{(1-\alpha)\lambda[(1-\alpha)\lambda + \alpha x]^{x-1} \exp\{-((1-\alpha)\lambda + \alpha x)\}}{x!} & (1-\alpha)\lambda + \alpha x \geq 0 \\ 0 & (1-\alpha)\lambda + \alpha x < 0 \end{cases} , \quad (3)$$

where GP denotes a generalized Poisson distribution with $E(X) = \lambda$ and $Var(X) = \frac{\lambda}{(1-\alpha)^2}$.

In addition, we allowed that two discrete traits, abdominal vertebrae number (mav) and caudal vertebrae number (mcv) could also with standard length (**CITATION**). This is because these are vertebral counts that run in parallel with the standard length measurement, along the anterior-posterior access of the fish; these vertebrae thus contribute to the length of the fish directly, and may evolve in a correlated fashion. If $Y_{k,ij}$ is one of the above traits,

then

$$Y_{k,ij} \sim \begin{cases} GP(\exp\{\mu_{k,ft_i} + \gamma_k Y_{K,ij}\}, \alpha_k), & W_{ij} = \text{Female} \\ GP(\exp\{\mu_{k,mt_i} + \gamma_k Y_{K,ij}\}, \alpha_k), & W_{ij} = \text{Male} \end{cases}. \quad (4)$$

For the other discrete traits, we set $\gamma_k = 0$ because we expect that trait counts are set during early ontogeny, and should not change with size in adult fish. Thus,

$$Y_{k,ij} \sim \begin{cases} GP(\exp\{\mu_{k,ft_i}\}, \alpha_k), & W_{ij} = \text{Female} \\ GP(\exp\{\mu_{k,mt_i}\}, \alpha_k), & W_{ij} = \text{Male} \end{cases}. \quad (5)$$

We point out that, for the discrete traits, the means are represented by $\exp\{\mu_{k,ft_i}\}$ and $\exp\{\mu_{k,mt_i}\}$ for ease of modeling.

In the above model descriptions, μ_{k,ft_i} and μ_{k,mt_i} model the time- t_i , sample-specific trait mean k for females and males, respectively. To account for the possibility that there is a time -dependent trend in μ_{k,ft_i} and μ_{k,mt_i} , we further set

$$\mu_{k,gt_i} = \beta_{0,k} + \beta_{1,k} t_i + u_{k,gt_i}, \quad (6)$$

for $g \in \{f, m\}$, where $\beta_{0,k}$ and $\beta_{1,k}$ are regression parameters of phenotype Y_k for each sex, and u_{k,gt_i} is the corresponding residual. To account for potential correlations between the residuals for a given trait k and sex g , we fit an Ornstein-Uhlenbeck (OU) process (Uhlenbeck and Ornstein (1930)). More specifically, we defined $du_{k,gt} = u_{k,g(t+dt)} - u_{k,gt}$, the change in $u_{k,gt}$ for a given trait k and sex g over a miniscule time period dt . The OU process is defined as

$$du_{k,gt} = -\kappa_k u_{k,gt} dt + \tau_k dW_t, \quad (7)$$

where κ_k is a parameter associated with the correlation between $u_{k,gt}$ and $u_{k,g(t+dt)}$, τ_k is the standard deviation of the OU process, and W_t is a standard Brownian motion. As shown in Uhlenbeck and Ornstein (1930), the closed form solution for the stochastic differential equation in (7) is

$$u_{k,gt_i} \stackrel{iid}{\sim} \mathcal{N}\left(u_{k,gt_{i-1}} \exp\{-\kappa_k(t_i - t_{i-1})\}, \frac{\tau_k^2(1 - \exp\{-2\kappa_k(t_i - t_{i-1})\})}{2\kappa_k}\right) \quad (8)$$

for $i = 2, \dots, T$. In a traditional OU process, the initial value u_{k,gt_1} is assumed to be a (potentially unknown) constant. This unknown constant can therefore be considered a latent variable, further justifying our Bayesian approach, which better incorporates prior information and uncertainty from missing data imputation in the estimate of the variable.

We discuss the procedure for estimating this value below. **DID THIS GET DISCUSSED?-YS**

Priors: To aid in the sampling procedure for the discrete phenotypes, we first had to transform the parameters of the generalized Poisson distribution onto the real number line in order to ensure our algorithm can properly sample from the posterior distribution of interest using STAN software. This was done by declaring $\phi_k = \log\left(\frac{\alpha_k - \max_{i,j}(-\lambda_{k,ij}/y_{k,ij})}{1 - \alpha_k}\right)$ where

$$\lambda_{k,ij} = \begin{cases} \exp(\mu_{k,ft_i} + \gamma_k Y_{K,ij}) & W_{ij} = \text{Female} \\ \exp(\mu_{k,mt_i} + \gamma_k Y_{K,ij}) & W_{ij} = \text{Male} \end{cases}.$$

We chose the following priors, designing them to be weakly informative such that the posterior distributions could be influenced by the data, if warranted. For $k = 1, \dots, K$,

$$\begin{aligned} u_{k,gt_1} &\overset{iid}{\sim} \mathcal{N}(0, \tau_{0,k}) \\ \sigma_k &\overset{iid}{\sim} \mathcal{N}(0, 10) I_{\{\sigma > 0\}} \\ \tau_k &\overset{iid}{\sim} \mathcal{N}(0, 10) I_{\{\tau > 0\}} \\ \tau_{0,k} &\overset{iid}{\sim} \mathcal{N}(0, 20) I_{\{\tau > 0\}} \\ \kappa_k &\overset{iid}{\sim} \mathcal{N}(0, 1) I_{\{\kappa_g > 0\}} \\ \gamma_k &\overset{iid}{\sim} \mathcal{N}(0, 5) \\ \beta_{0,kg} &\overset{iid}{\sim} \mathcal{N}(0, 100) \\ \beta_{1,kg} &\overset{iid}{\sim} \mathcal{N}(0, 3) \end{aligned} \tag{9}$$

We also note that, for the discrete phenotypes in equations (4) and (5), there is no σ_k , and it is not sampled, and for the continuous phenotypes in equation (2), there is no ϕ_k and it is not sampled.

We follow the method outlined in (Zhou and Reiter?) to obtain R draws from the posterior distribution of the outlined model parameters given our observed data and imputed values. More specifically, for the j^{th} imputed data set where $j = 1, \dots, M$, we obtain $\frac{R}{M}$ draws from the posterior distribution using an MCMC algorithm with a sufficient burnin period, and then we combine these M MCMC draws to say that we have a total of R draws from the overall posterior distribution of interest, which can then be used to assess the presence of sexual dimorphism for a given trait.

After running these models, we have posterior distributions of all the model parameters of interest. From these, we can obtain samples from the posterior distribution of mean trait values for each trait for males and females, using equation 6. We use these values for the following analyses.

2.6 Quantifying sexual dimorphism, and testing for increased sexual dimorphism through time.

We identify sexual dimorphism first by calculating the difference in mean trait size for males and females at each time for phenotype k ($\mu_{k,m,t_i} - \mu_{k,f,t_i}$) for $i = 1, \dots, T$ where, for the continuous phenotypes, the mean trait sizes for each sex μ_{k,m,t_i} and μ_{k,f,t_i} are calculated using (6). For the discrete phenotypes, we note that in (4) and (5) the mean trait size is $\lambda_{k,m,t_i} = \exp(\mu_{k,m,t_i})$ and $\lambda_{k,f,t_i} = \exp(\mu_{k,f,t_i})$ for males and females, respectively, which is the value we use in our analysis. For simplicity, we will use μ_{k,m,t_i} and μ_{k,f,t_i} as the notation for mean size for both discrete and continuous traits for the rest of this discussion. From our MCMC algorithm, we obtain M samples from the posterior distribution of $\mu_{k,m,t_i} - \mu_{k,f,t_i}$ to use in our analysis.

Recall that we predicted that sexual dimorphism should increase through time in Lineage II, following ecological release from predators. However, this change in dimorphism make be increasing at a non-constant rate, as pointed out by the inclusion of the OU process. We assess for dimorphism by calculating a Kendall's τ coefficient (KENDALL (1938)). Kendall's τ assesses the ordinal association between a set of bivariate observations, where $\tau > 0$ indicates concordance between the observations (i.e., as x increases, y also tends to increase.)

For our analysis, we calculate $\boldsymbol{\tau}_k = \{\tau_{k,r} : r = 1, \dots, R\}$ for trait k where τ_r is the estimate of the Kendall's τ correlation for $\mu_{k,m,t_i} - \mu_{k,f,t_i}$ versus time t_i for the r^{th} MCMC sample from the posterior distribution. The posterior probability of sexual dimorphism for trait k can be estimated as the proportion of values in $\boldsymbol{\tau}_k$ that are greater than 0 ($\frac{1}{R} \sum_{r=1}^R I(\tau_{k,r} > 0)$). We can also assess the strength of the dimorphism by calculating the proportion of posterior samples that are greater than a prespecified threshold (0.5??, idk what this could be.) -MS

3 Results

WE NEED RESULTS SECTION DESCRIBING THE RESULTS OF AKHIL'S MULTIPLE IMPUTATION, BOTH THE TESTS OF HOW WELL THE MODEL WORKED CLASSIFYING MODEL SAMPLES, AND SUMMARY STATISTICS OF FOSSIL IMPUTATION RESULTS -YS

3.1 Sexual Dimorphism

Table ?? shows the posterior probability of the differences in the means between male and female specimens at each time point. Probabilities near 0.5 indicate very little difference in the means whereas probabilities far from 0.5 indicate sexual dimorphism with values of 0

and 1 indicating larger mean values for females and males, respectively. These results are shown graphically in figure 2.

Figure 1 shows the posterior mean difference for males versus females (values above 0 indicate means that were greater for males versus females). The full posterior distributions over time for all traits are shown in the appendix.

Traits such as standard length (stl), anal fin ray (maf), dorsal fin ray (mdf), premaxilla (pmx), and dorsal spine 1 (ds1) demonstrate constant sexual dimorphism with all but the last having learger mean values in male sepcimen. Other traits such as abdominal vertebra (mav), caudal vertebra (mcv), and pelvic spine length (lps) don't appear to have any discernable sexual dimorphism in the means. Dorsal spine 3 (ds3) exhibits sexual dimorphism that changes over time. The mean number of dorsal spine 3 begins larger for females for the earliest observed time periods. Over time, however, this switches and the male specimens exhibit larger mean values for the latest observed time periods.

Yoel's interpretation of the three paragraphs above. Male and female *G. doryssus* differ for some traits, indicating detectable sexual dimorphism. This is evidenced by traits with substantial differences in male and female posterior means (i.e., deviation from 0 in Figure 1), supported by posterior probabilities that deviate from 0.5 (Figure 2). For example, males are larger than females by 3-8mm on average through time (stl panel in Figure 1), with a posterior probability for that mean difference above 70 percent through time (Figure 2). In contrast, the number of abdominal vertebrae (mav) fluctuates about 0 (Figure 1), with posterior probabilities fluctuating about 50 percent through time (Figure 2). Table ?? in the Supplementary Material summarizes the posterior probabilities that male means differ from female means by trait and sample.

can we move mu-diff-plot and prob0-plot here?

3.2 Changes over time

Table ?? shows the probability that the posterior distribution of the differences in the mean is greater than the posterior distribution of the differences at the first time point. Values near 0.5 indicate very little difference between the distributions whereas values closer to 0 and 1 indicate changes in the distributions with values of 1 meaning the difference in means has shifted towards males having a larger mean and values of 0 indicating the difference in means has shifted towards larger means in females. These results are shown graphically in figure 3.

The amount of sexual dimorphism over time does not change substantially for a majority of the trait observed here (i.e. cle, ds1, ds2, ect, lps, lpt, mav, mcv, pmx, stl). Traits that

trend away from the mean difference at the first observed time point include dorsal spine 3 (ds3), anal fin ray (maf), and dorsal fin ray (mdf).

The posterior mean of the mean number of dorsal spine rays at the first observed time point is 2.29 for males and for females it is 2.45. At the last observed time point, the average number for males and female both dropped to 1.265 and 1.185 for males and females, respectively. This resulted in a mean number of dorsal spine 3 lost by males of 1.027 and for females it was 1.264. This resulted in a change of the mean difference from time point 1 to time point 18 of 0.236. Basically, males and females both lowered the mean number of dorsal spine 3, but females lowered their mean more than the males.

We also observed a change in the differences between males and females for the number of bones in the anal fin ray (maf) and the number of bones in the dorsal fin ray. The difference in the means of males versus females for anal fin ray bones changed by 0.152 over the course of the observed time periods. This change was driven mostly by the change in females. At the first observed time period they had on average 8.291 bones dropping to 8.170 over the 18 time periods observed. Whereas for males the change in means rose only from 8.518 to 8.549, about 0.0316 bones on average.

A similar change in the difference of the means over time was observed for the number of bones in the dorsal fin (mdf). However, unlike maf, this change in sexual dimorphism was driven entirely by the males. The mean change for females over the 18 observed time periods was only 0.0055 with the average number of dorsal fin bones for females starting at 9.287 and the final observed mean of 9.281 resulting in almost no change in the mean. For males, the average number of dorsal fin bones at the first time point was about 9.568 dropping to 9.734 over the course of the observed time periods for a gain of 0.166 bones on average.

Yoel's interpretation of the five paragraphs above. Figure 3 shows the posterior probability that the mean male-female difference at time t is different from the male-female difference at time zero. In other words, Figure 3 plots whether the sexual dimorphism changes in subsequent samples, always relative to the first sample. The amount of sexual dimorphism over time does not change substantially for a majority of the traits (i.e. cle, ds1, ds2, ect, lps, lpt, mav, mcv, pmx, stl; Figure 3). Traits that change in dimorphism are anal fin ray (maf), and dorsal fin ray (mdf), and dorsal spine 3 (ds3).

For example, females at time zero averaged 8.29 rays in the anal fin, dropping to 8.17 rays in the final sample. Males averaged 8.52 anal fin rays in the first sample and 8.55 in the last sample. Thus, the difference between males and females started at 0.23 and ended at 0.38, an increase in sexual dimorphism. In contrast, the sign on dimorphism flipped for ds3. The posterior mean length of the third dorsal spine is 2.29mm for males and 2.45mm for females. By the end of the sequence, mean ds3 for males was 1.27 for males and 1.19 for females. Both sexes evolved reduction of ds3, but females lowered their mean more than the males.

This resulted in a flip in dimorphism, from larger females to larger males, though both sexes evolved trait reduction. BUT DIMORPHISM SHRUNK THEN, AS THE DIFFERENCE BETWEEN MALES AND FEMALES IS NOW SMALLER??

time	cle	ds1	ds2	ds3	ect	lps	lpt	maf	mav	mcv	mdf	pmx	stl
1	0.913	0.215	0.359	0.203	0.865	0.428	0.853	0.944	0.391	0.507	0.959	0.948	0.883
2	0.942	0.212	0.325	0.180	0.891	0.404	0.853	0.948	0.520	0.520	0.963	0.967	0.908
3	0.843	0.207	0.249	0.153	0.770	0.279	0.803	0.965	0.289	0.525	0.977	0.912	0.777
4	0.890	0.210	0.249	0.201	0.830	0.372	0.741	0.977	0.435	0.589	0.986	0.935	0.831
5	0.954	0.211	0.211	0.195	0.909	0.377	0.756	0.985	0.533	0.622	0.992	0.975	0.921
6	0.885	0.211	0.134	0.171	0.820	0.291	0.686	0.991	0.645	0.456	0.996	0.949	0.811
7	0.812	0.211	0.124	0.239	0.760	0.340	0.617	0.994	0.224	0.717	0.999	0.879	0.747
8	0.928	0.210	0.135	0.258	0.885	0.387	0.706	0.994	0.342	0.730	1.000	0.969	0.872
9	0.899	0.213	0.145	0.304	0.857	0.406	0.715	0.995	0.521	0.756	1.000	0.940	0.845
10	0.954	0.217	0.235	0.555	0.940	0.571	0.810	0.997	0.454	0.719	1.000	0.976	0.935
11	0.913	0.211	0.162	0.476	0.875	0.388	0.703	0.997	0.363	0.657	1.000	0.957	0.864
12	0.949	0.221	0.262	0.726	0.929	0.585	0.803	0.997	0.462	0.595	1.000	0.968	0.926
13	0.904	0.220	0.260	0.789	0.885	0.598	0.795	0.998	0.470	0.370	1.000	0.929	0.872
14	0.925	0.220	0.280	0.883	0.906	0.659	0.854	0.997	0.526	0.472	1.000	0.958	0.898
15	0.880	0.225	0.283	0.839	0.849	0.617	0.796	0.997	0.490	0.398	1.000	0.919	0.834
16	0.953	0.216	0.276	0.931	0.931	0.614	0.831	0.997	0.414	0.541	1.000	0.975	0.925
17	0.803	0.219	0.232	0.832	0.765	0.383	0.655	0.996	0.569	0.758	1.000	0.854	0.751
18	0.780	0.212	0.225	0.817	0.726	0.297	0.558	0.995	0.705	0.722	0.999	0.859	0.717

time	cle	ds1	ds2	ds3	ect	lps	lpt	maf	mav	mcv	mdf	pmx	stl
1	0.500	0.500	0.500	0.500	0.500	0.500	0.500	0.500	0.500	0.500	0.500	0.500	0.500
2	0.514	0.504	0.509	0.495	0.512	0.508	0.517	0.495	0.396	0.490	0.495	0.511	0.513
3	0.636	0.514	0.559	0.516	0.628	0.601	0.602	0.475	0.523	0.480	0.476	0.626	0.641
4	0.563	0.509	0.544	0.459	0.558	0.539	0.672	0.456	0.436	0.450	0.458	0.556	0.562
5	0.543	0.507	0.551	0.417	0.539	0.522	0.687	0.436	0.389	0.425	0.439	0.537	0.544
6	0.618	0.512	0.589	0.415	0.613	0.579	0.716	0.415	0.317	0.522	0.419	0.612	0.620
7	0.591	0.510	0.601	0.364	0.589	0.564	0.712	0.379	0.546	0.382	0.383	0.588	0.592
8	0.539	0.507	0.579	0.324	0.536	0.514	0.683	0.373	0.478	0.368	0.378	0.537	0.540
9	0.524	0.506	0.586	0.299	0.521	0.510	0.636	0.355	0.408	0.340	0.359	0.523	0.522
10	0.379	0.497	0.544	0.203	0.377	0.400	0.578	0.321	0.438	0.359	0.324	0.385	0.373
11	0.531	0.508	0.605	0.226	0.528	0.517	0.685	0.301	0.528	0.403	0.303	0.530	0.533
12	0.363	0.492	0.547	0.150	0.360	0.386	0.566	0.284	0.439	0.436	0.284	0.369	0.358
13	0.373	0.495	0.555	0.133	0.372	0.386	0.561	0.269	0.432	0.575	0.268	0.378	0.371

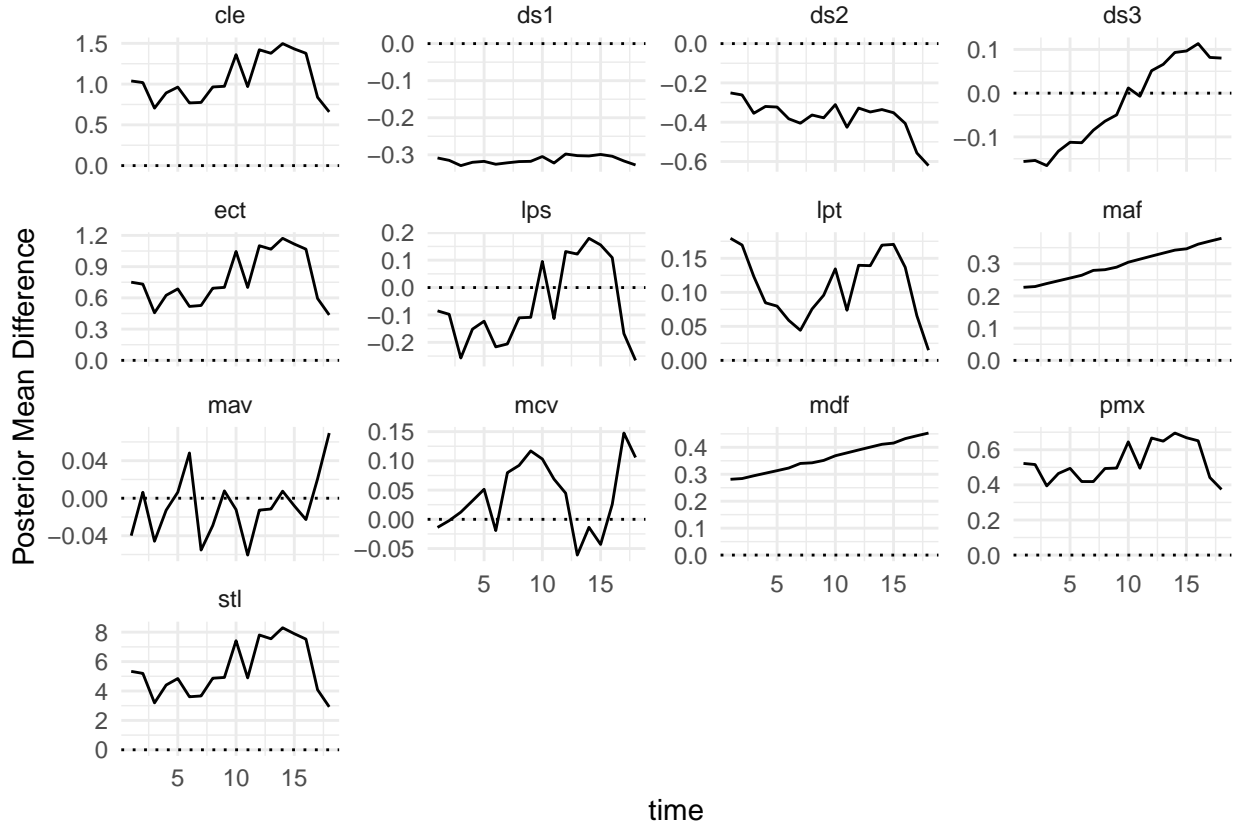


Figure 1: Posterior mean difference between males and females, in UNITS?. Values above 0 indicate larger male means

time	cle	ds1	ds2	ds3	ect	lps	lpt	maf	mav	mcv	mdf	pmx	stl
14	0.326	0.496	0.548	0.102	0.326	0.349	0.514	0.255	0.399	0.514	0.253	0.334	0.323
15	0.365	0.492	0.552	0.107	0.365	0.373	0.502	0.250	0.433	0.554	0.247	0.368	0.367
16	0.361	0.497	0.574	0.084	0.360	0.381	0.570	0.234	0.462	0.463	0.229	0.369	0.356
17	0.561	0.504	0.629	0.116	0.559	0.542	0.669	0.226	0.364	0.313	0.219	0.559	0.565
18	0.625	0.512	0.648	0.121	0.617	0.596	0.735	0.220	0.281	0.356	0.212	0.622	0.627

posterior mean difference for males versus females (values above 0 indicate means that were greater for males versus females)

4 Discussion, Future work and conclusions

We predicted that release from predators would result in niche expansion and increased sexual dimorphism, based on several studies of modern stickleback. For example, in lakes

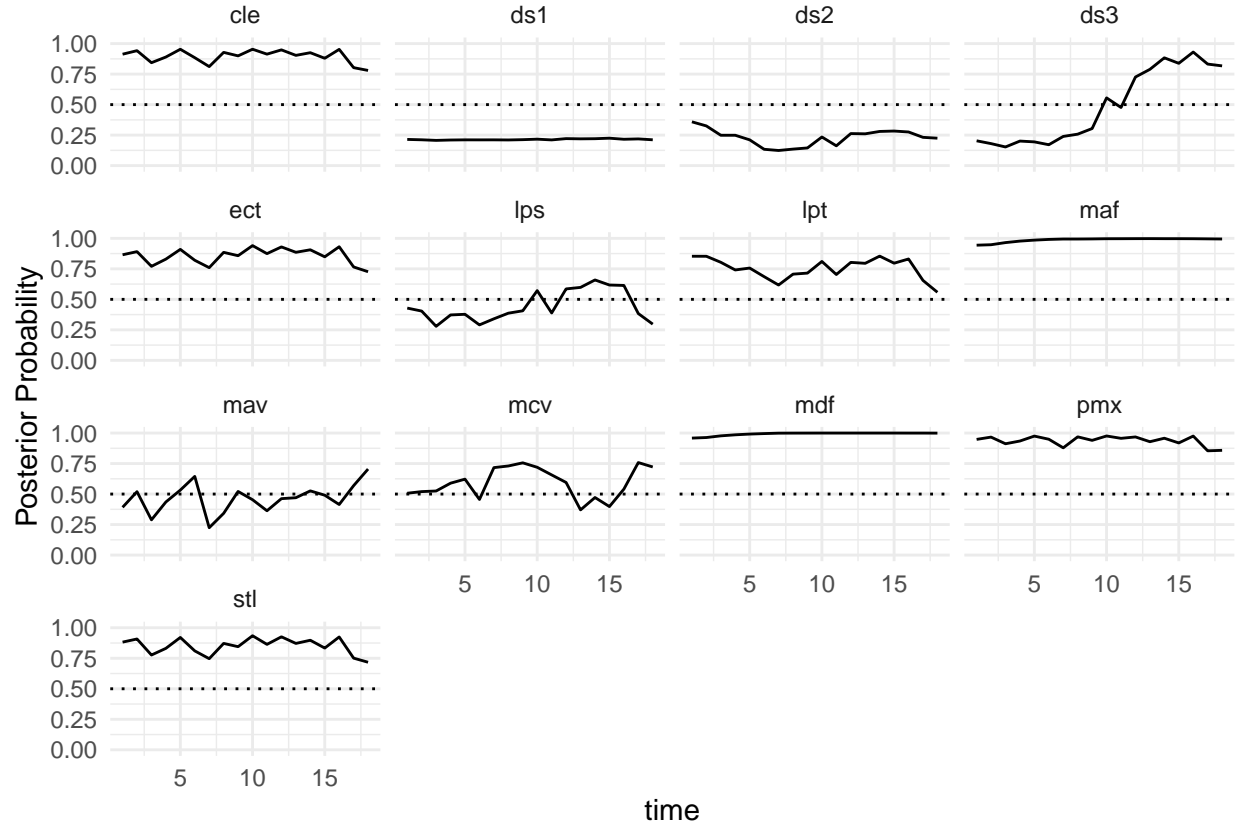


Figure 2: Posterior probabilities that the male posterior mean is larger than the female posterior mean

where sculpin competitors are absent and stickleback (Roesti et al. 2023) See Spoljaric and Reimchen 2008, page 512 right column for references and discussion of differences between benthic males and limnetic females. Male stickleback are benthic and littoral (Wootton 1976)... Reimchen papers in general good for this section. Moreover, tooth wear data from the lineage II sequence suggest that individuals in this lineage began eating more planktonic prey over time, expanding toward an open-water niche from the benthic, bottom-feeding niche they started with (Purnell et al. 2007). That this expansion into open water by lineage II coincided with armor reduction is further indicative of a limnetic system with fewer salmonid piscivores (Schluter and McPhail (1992); Vamosi and Schluter (2004); Roesti et al. (2023)).

Acknowledgements

We thank O. Abughoush, S. Blain, A. Chaudhary, M. Islam, F. Joaquin, C. Lawson-Weinert, R. Sullivan, J. Tien, M.P. Travis, and W. Shim for help with data collection. We thank D.

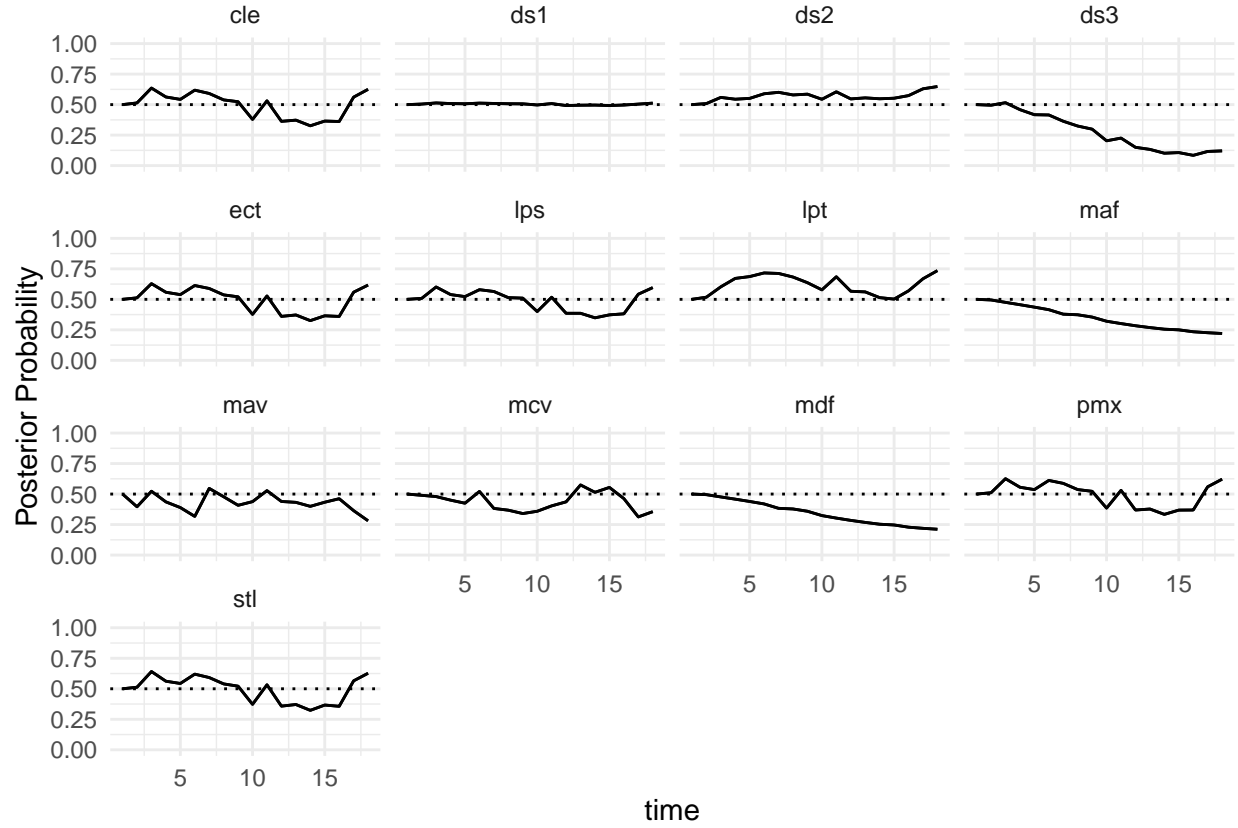


Figure 3: The Posterior Probability that male-female differences in subsequent samples are different from male-female differences in the initial sample. Values near 0.5 indicate little difference between the distributions. Values closer to 0 indicate that the difference in means has shifted towards larger means in females. Values closer to 1 indicate that the difference in means has shifted toward larger means in males.

Schluter and S. Blain for loaning specimens and sharing data. We thank K. Swagel and C. McMahan of the Field Museum for assistance with specimen x-rays. This research was supported by NSF grants BSR-8111013, EAR-9870337, and DEB-0322818, the Center for Field Research (Earthwatch), and the National Geographic Society (2869-84) to MAB. It was also supported by NSF grants DEB-1456462 and EAR-2145830 to YES. And NSF DMS-2015374 (GJM)

Supplementary Material

All code for reproducing the analyses in this paper is publicly available at <https://github.com/Akhil-Ghosh/SticklebackProject>

DIC results here.

4.1 Figures

5 References

- Aguirre, W E, K Walker, and S Gideon. 2014. “Tinkering with the Axial Skeleton: Vertebral Number Variation in Ecologically Divergent Threespine Stickleback Populations.” *Biological Journal of the Linnean Society* 113 (1): 204–19.
- Baumgartner, J V, M A Bell, and P H Weinberg. 1988. “Body Form Differences Between the Enos Lake Species Pair of Threespine Sticklebacks (*Gasterosteus Aculeatus* Complex).” *Canadian Journal of Zoology* 66 (2): 467–74.
- Bell, M A. 2009. “Implications of a Fossil Stickleback Assemblage for Darwinian Gradualism.” *Journal of Fish Biology* 75 (8): 1977–99.
- Bell, M A, J V Baumgartner, and E C Oslen. 1985. “Patterns of Temporal Change in Single Morphological Characters of a Miocene Stickleback Fish.” *Paleobiology* 11: 258–71.
- Bell, M A, G Orti, J A Walker, and J P Koenings. 1993. “Evolution of Pelvic Reduction in Threespine Sticklebacks: A Test of Competing Hypotheses.” *Evolution* 47: 906–14.
- Bell, M A, M P Travis, and D M Blouw. 2006. “Inferring Natural Selection in a Fossil Threespine Stickleback.” *Paleobiology* 32 (4): 562–77.
- Blain, S A. 2022. *Evolutionary Outcomes of Interactions Among Phenotypes in Post-Glacial Lakes*. University of British Columbia, Canada.
- Bolnick, D I. 2011. “Sympatric Speciation in Threespine Stickleback: Why Not?” *International Journal of Ecology* 2011: 1–15.
- Bolnick, D I, and M Doebeli. 2003. “Sexual Dimorphism and Adaptive Speciation: Two Sides of the Same Ecological Coin.” *Evolution* 57 (11): 2433–49.
- Bolnick, D I, and O L Lau. 2008. “Predictable Patterns of Disruptive Selection in Stickleback in Postglacial Lakes.” *The American Naturalist* 172 (1): 1–11.
- Bowne, P S. 1994. “Systematics and Morphology of the *Gasterosteiformes*.” In *The Evolutionary Biology of the Threespine Stickleback*, edited by M A Bell and S A Foster. Oxford, UK: Oxford University Press.
- Butler, Sawyer, M A, and J B Losos. 2007. “Sexual Dimorphism and Adaptive Radiation in *Anolis* Lizards.” *Nature* 447 (7141): 202–5.
- Buuren, Stef van, and Karin Groothuis-Oudshoorn. 2011. “Mice: Multivariate Imputation by Chained Equations in r.” *Journal of Statistical Software* 45 (3): 1–67. <https://doi.org/10.18637/jss.v045.i03>.
- Cerasoni, J N, M A Bell, and Y E Stuart. 2024. “Geology, Microstratigraphy, and Paleontology of Truckee Formation Lacustrine Diatomite Deposits Near Hazen, Nevada, USA, with Emphasis on Fossil Stickleback Fish.” *PaleoBios* 41: 1–15.
- Cooper, I A, R T Gilman, and J W Boughman. 2011. “Sexual Dimorphism and Speciation on Two Ecological Coins: Patterns from Nature and Theoretical Predictions.” *Evolution*

- 65 (9): 2553–71.
- De Lisle, S P, S Paiva, and L Rowe. 2018. “Habitat Partitioning During Character Displacement Between the Sexes.” *Biology Letters* 14: 20180124.
- De Lisle, S P, and L Rowe. 2015. “Ecological Character Displacement Between the Sexes.” *The American Naturalist* 186: 693–707.
- . 2017. “Disruptive Natural Selection Predicts Divergence Between the Sexes During Adaptive Radiation.” *Ecology and Evolution* 7: 3590–3601.
- Godfrey, L R, S K Lyon, and M R Sutherland. 1993. “Sexual Dimorphism in Large-Bodied Primates: The Case of the Subfossil Lemurs.” *American Journal of Physical Anthropology* 90: 315–34.
- Hendry, A P, D I Bolnick, D Berner, and C L Peichel. 2009. “Along the Speciation Continuum in Sticklebacks.” *Journal of Fish Biology* 75 (8): 2000–2036.
- Herrmann, N C, J T Stroud, and J B Losos. 2021. “The Evolution of ‘Ecological Release’ into the 21st Century.” *Trends in Ecology and Evolution* 36 (3): 206–15.
- Hone, D W E, and J C Mallon. 2017. “Protracted Growth Impedes the Detection of Sexual Dimorphism in Non-Avian Dinosaurs.” *Palaeontology* 60 (4): 535–45.
- Hunt, G, M A Bell, and M P Travis. 2008. “Evolution Toward a New Adaptive Optimum: Phenotypic Evolution in a Fossil Stickleback Lineage.” *Evolution* 62 (3): 700–710.
- KENDALL, M. G. 1938. “A NEW MEASURE OF RANK CORRELATION.” *Biometrika* 30 (1-2): 81–93. <https://doi.org/10.1093/biomet/30.1-2.81>.
- Koscinski, K, and S Pietraszewski. 2004. “Methods to Estimate Sexual Dimorphism from Unsexed Samples: A Test with Computer Generated Samples.” *Przegląd Antropologiczny - Anthropological Review* 67: 33–55.
- Little, R. J. A., and D. B. Rubin. 2002. *Statistical Analysis with Missing Data*. Wiley Series in Probability and Mathematical Statistics. Probability and Mathematical Statistics. Wiley. <http://books.google.com/books?id=aYPwAAAAMAAJ>.
- Mallon, J C. 2017. “Recognizing Sexual Dimorphism in the Fossil Record: Lessons from Nonavian Dinosaurs.” *Paleobiology* 43 (3): 495–507.
- Parent, C E, and B J Crespi. 2009. “Ecological Opportunity in Adaptive Radiation of Galapagos Endemic Land Snails.” *The American Naturalist* 174: 898–905.
- Pfennig, D W, and K S Pfennig. 2012. *Evolution’s Wedge: Competition and the Origins of Diversity*. University of California Press, Berkeley, USA.
- Reimchen, T E. 1994. “Predators and Morphological Evolution in Threespine Stickleback.” In *The Evolutionary Biology of the Threespine Stickleback*, edited by M A Bell and S A Foster. Oxford, UK: Oxford University Press.
- Reimchen, T E, and P Nosil. 2004. “Variable Predation Regimes Predict the Evolution of Sexual Dimorphism in a Population of Threespine Stickleback.” *Evolution* 58 (6): 1274–81.
- Roesti, M, J S Groh, S A Blain, M Huss, P Rassias, D I Bolnick, Y E Stuart, C L Peichel,

- and D Schluter. 2023. “Species Divergence Under Competition and Shared Predation.” *Ecology Letters* 26: 111–23.
- Saitta, T, M T Stockdale, N R Longrich, V Bonhomme, M J Benton, I C Cuthill, and P J Makovicky. 2020. “An Effect Size Statistical Framework for Investigating Sexual Dimorphism in Non-Avian Dinosaurs and Other Extinct Taxa.” *Biological Journal of the Linnean Society* 131 (2): 231–73. <https://doi.org/10.1093/biolinnean/blaa105>.
- Schindelin, J, I Arganda-Carreras, E Frise, V Kaynig, M Longair, T Pietzsch, S Preibisch, C Rueden, S Saalfeld, and B Schmid. 2012. “Fiji: An Open-Source Platform for Biological-Image Analysis.” *Nature Methods* 9: 976–682.
- Schluter, D, and J D McPhail. 1992. “Ecological Character Displacement and Speciation in Sticklebacks.” *The American Naturalist* 140 (1): 85–108.
- Schoener, T W. 1968. “The Anolis Lizards of Bimini: Resource Partitioning in a Complex Fauna.” *Ecology* 29: 704–26.
- Shine, R. 1989. “Ecological Causes for the Evolution of Sexual Dimorphism: A Review of the Evidence.” *The Quarterly Review of Biology* 64 (4): 419–61.
- Siddiqui, R, S Swank, A Ozark, F Joaquin, M P Travis, C D McMahan, M A Bell, and Y E Stuart. 2024. “Inferring the Evolution of Reproductive Isolation in a Lineage of Fossil Threespine Stickleback, *Gasterosteus Doryssus*.” *Proceedings of the Royal Society B* 291: 20240337.
- Stuart, Y E, J W Sherwin, A Kamath, and T Veen. 2021. “Male and Female Anolis Carolinensis Maintain Their Dimorphism Despite the Presence of Novel Interspecific Competition.” *Evolution* 75 (11): 2708–16.
- Stuart, Y E, M P Travis, and M A Bell. 2020. “Inferred Genetic Architecture Underlying Evolution in a Fossil Stickleback Lineage.” *Nature Ecology and Evolution* 4 (11): 1549–57.
- Stuart, Y E, T Veen, J N Weber, D Hanson, M Ravinet, B K Lohman, C J Thompson, et al. 2017. “Contrasting Effects of Environment and Genetics Generate a Continuum of Parallel Evolution.” *Nature Ecology and Evolution* 1 (6): 158.
- Uhlenbeck, G E, and L S Ornstein. 1930. “On the Theory of the Brownian Motion.” *Phys. Rev.* 36 (September): 823–41. <https://doi.org/10.1103/PhysRev.36.823>.
- Vamosi, S M, and D Schluter. 2004. “Character Shifts in the Defensive Armor of Sympatric Sticklebacks.” *Evolution* 58: 376–85.
- Voje, K L, M A Bell, and Y E Stuart. 2022. “Evolution of Static Allometry and Constraint on Evolutionary Allometry in a Fossil Stickleback.” *Journal of Evolutionary Biology* 35 (3): 423–38.
- Zhou, X, and J Reiter. 2010. “A Note on Bayesian Inference After Multiple Imputation.” *The American Statistician* 64 (2): 159–63.

cle: No OU – No Trend

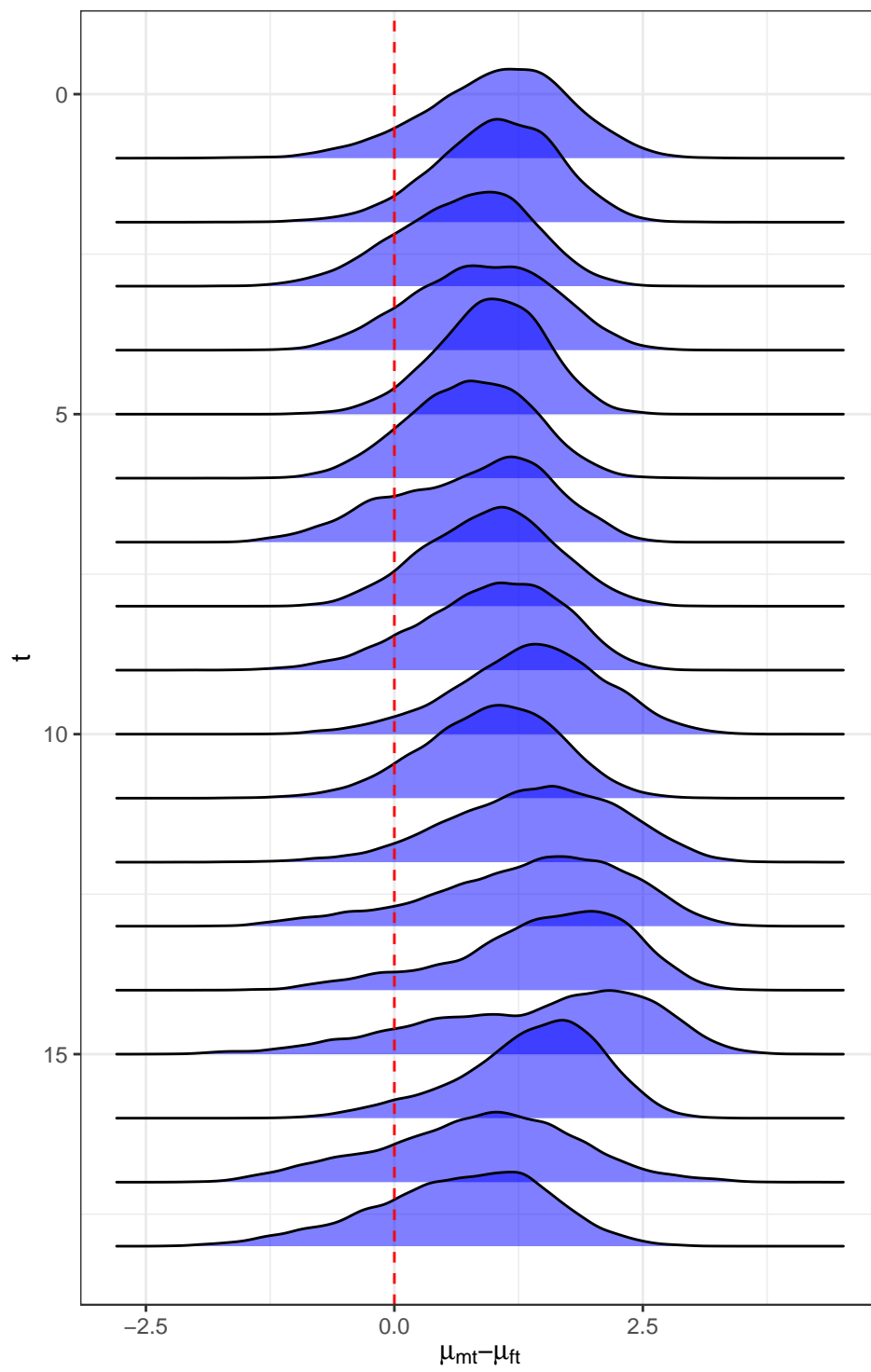


Figure 4: cle

ds1: No OU – No Trend

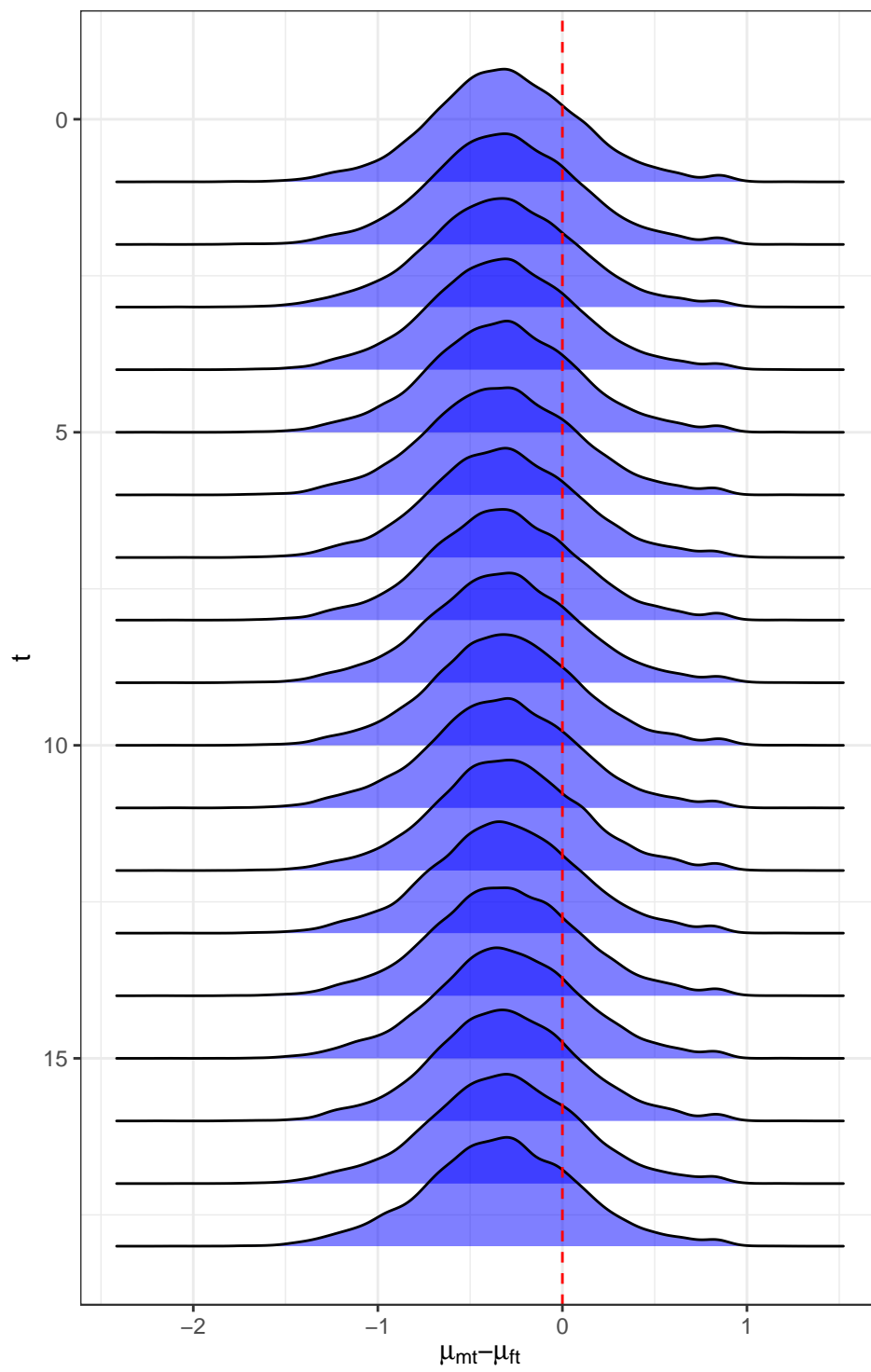


Figure 5: ds1

ds2: No OU – Trend

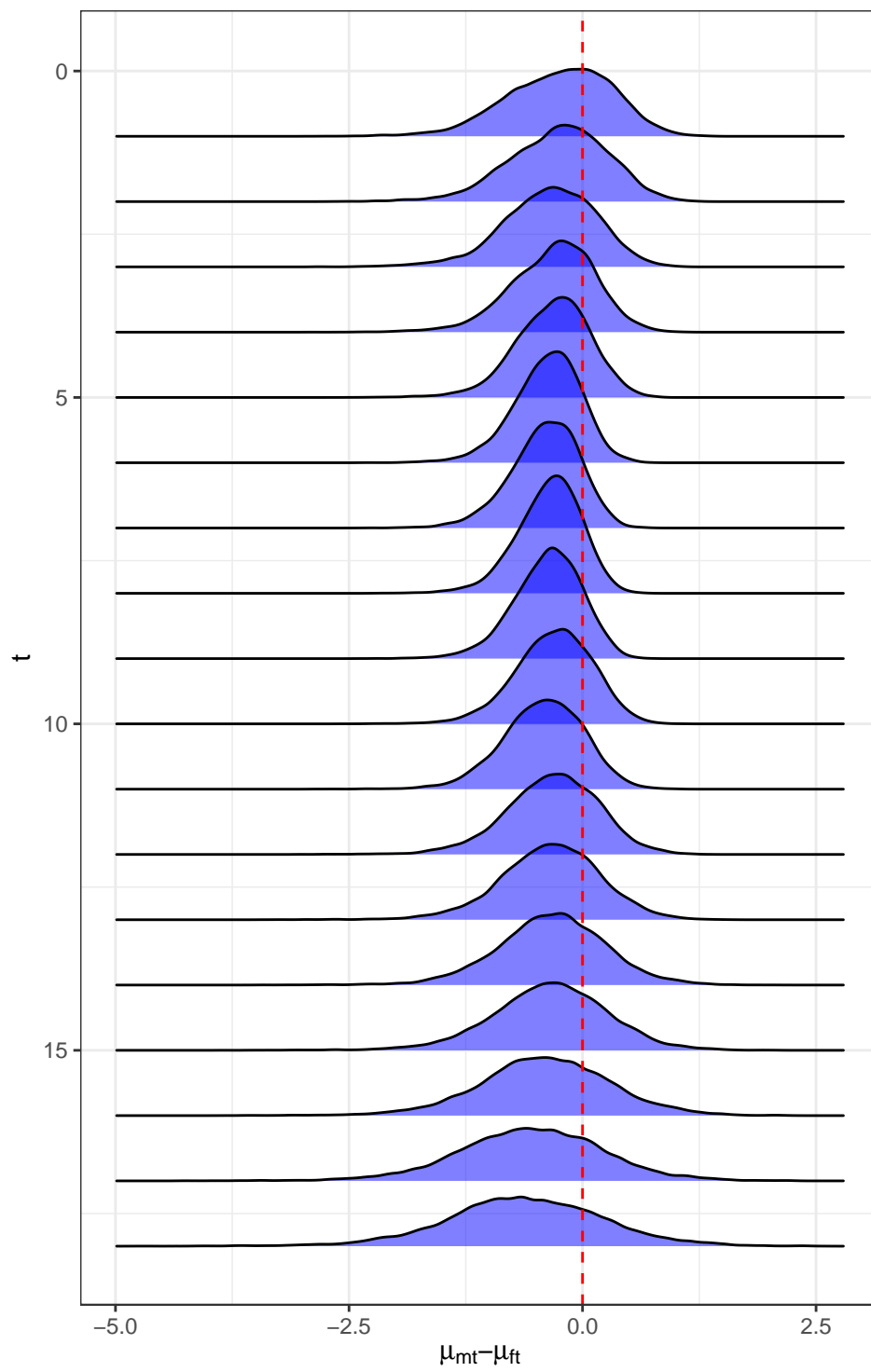


Figure 6: ds2

ds3: No OU – Trend

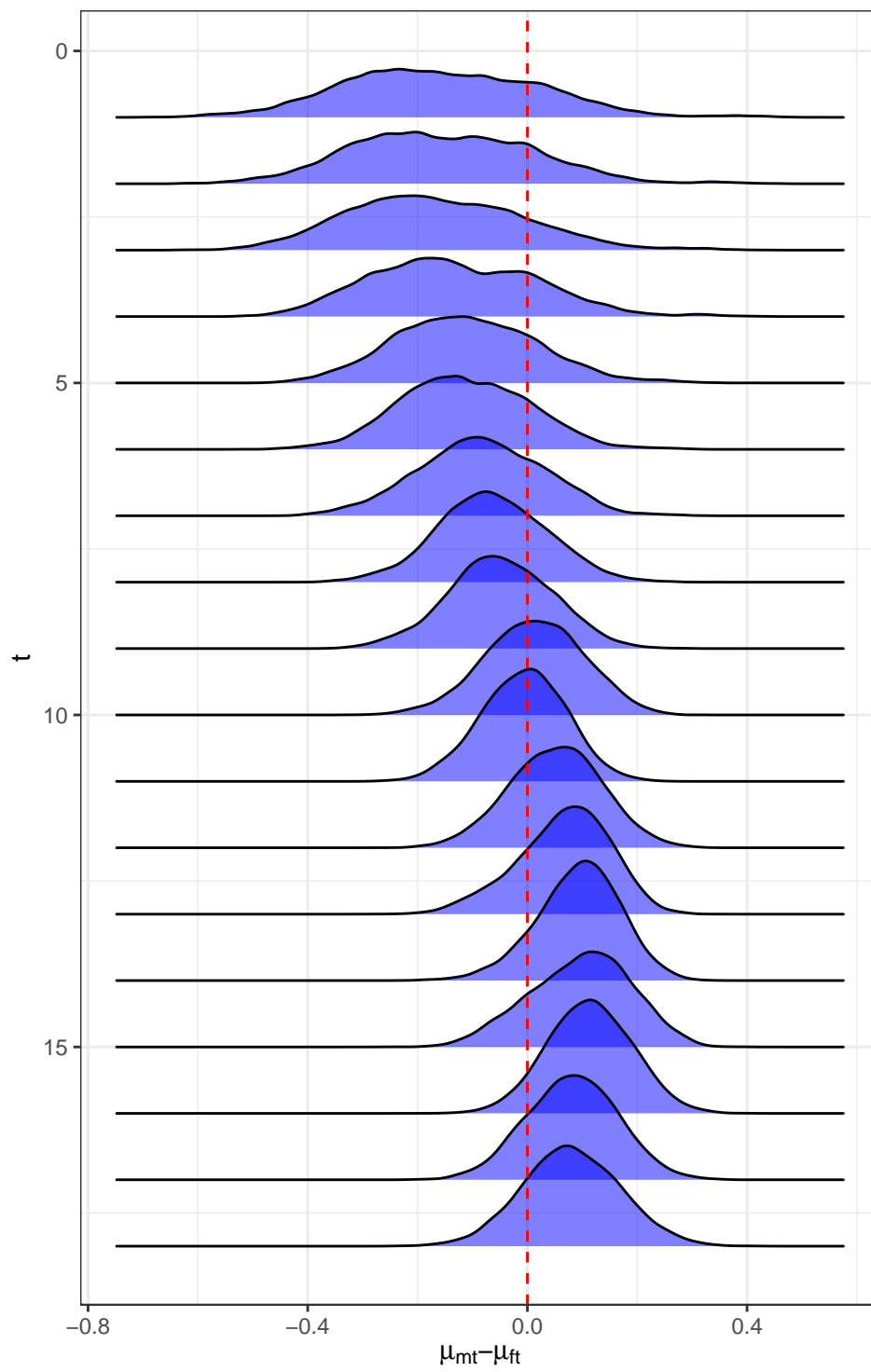


Figure 7: ds3

ect: No OU – Trend

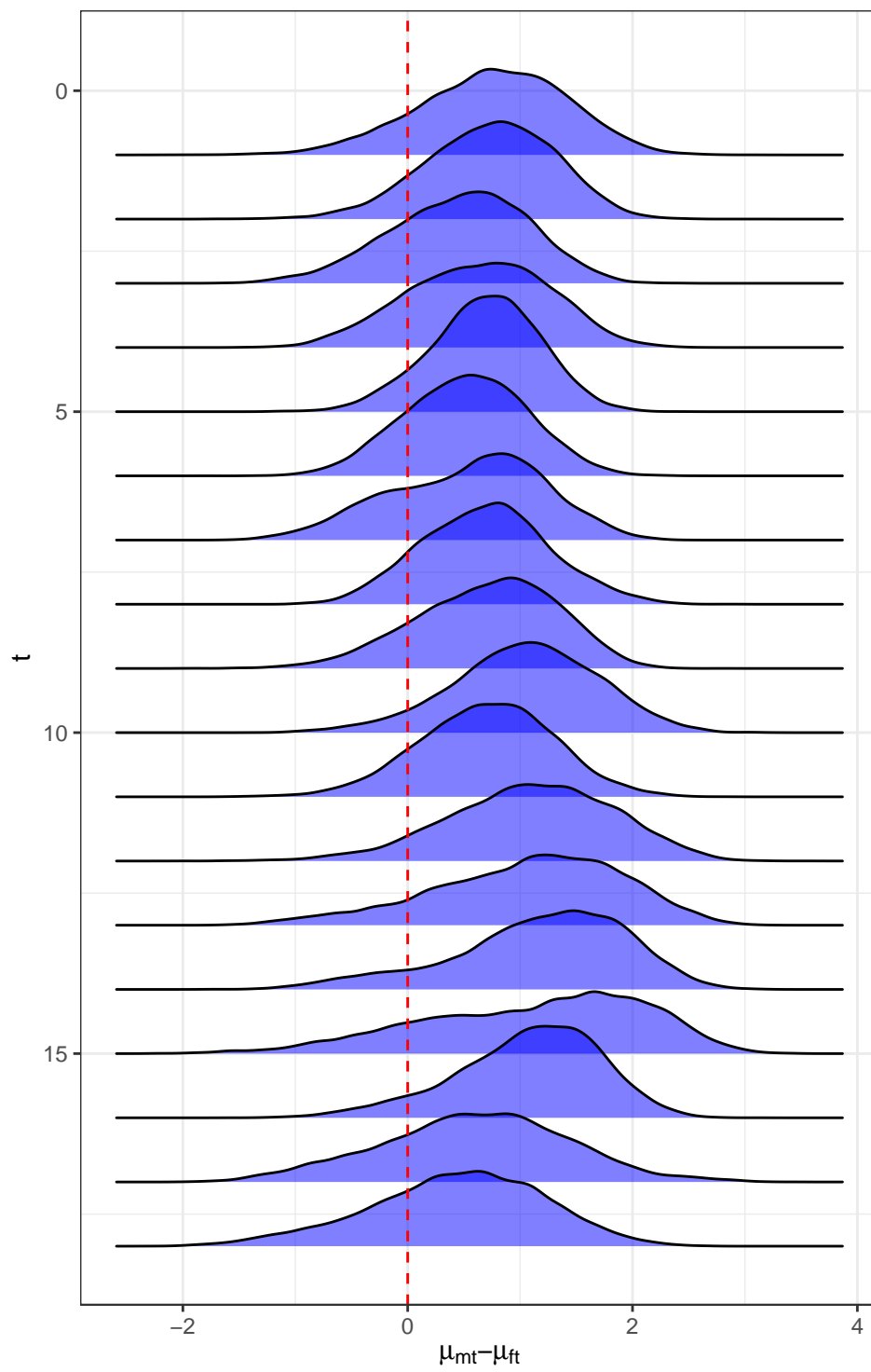


Figure 8: ect

lps: No OU – No Trend

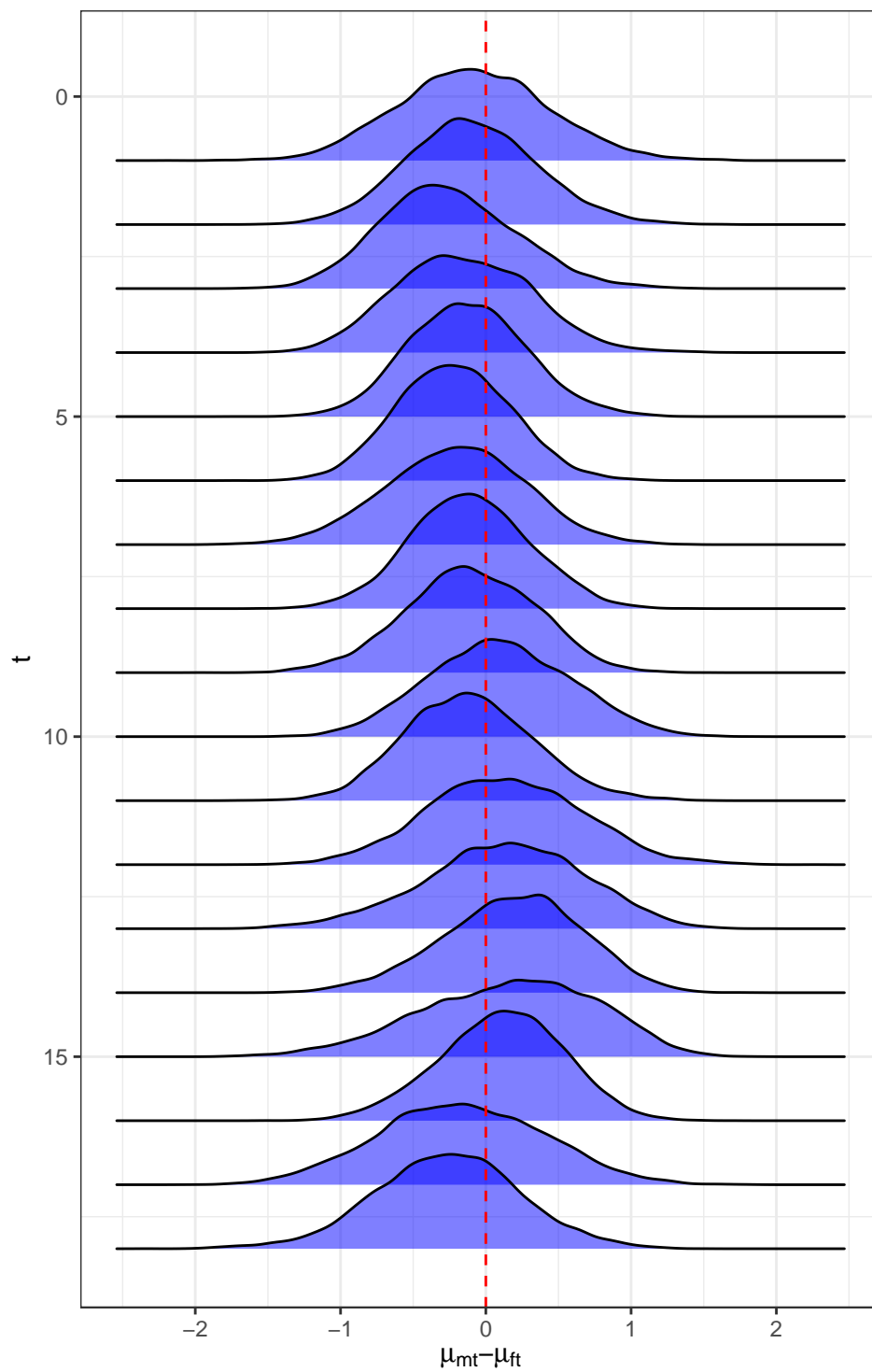


Figure 9: lps

lpt: OU – No Trend

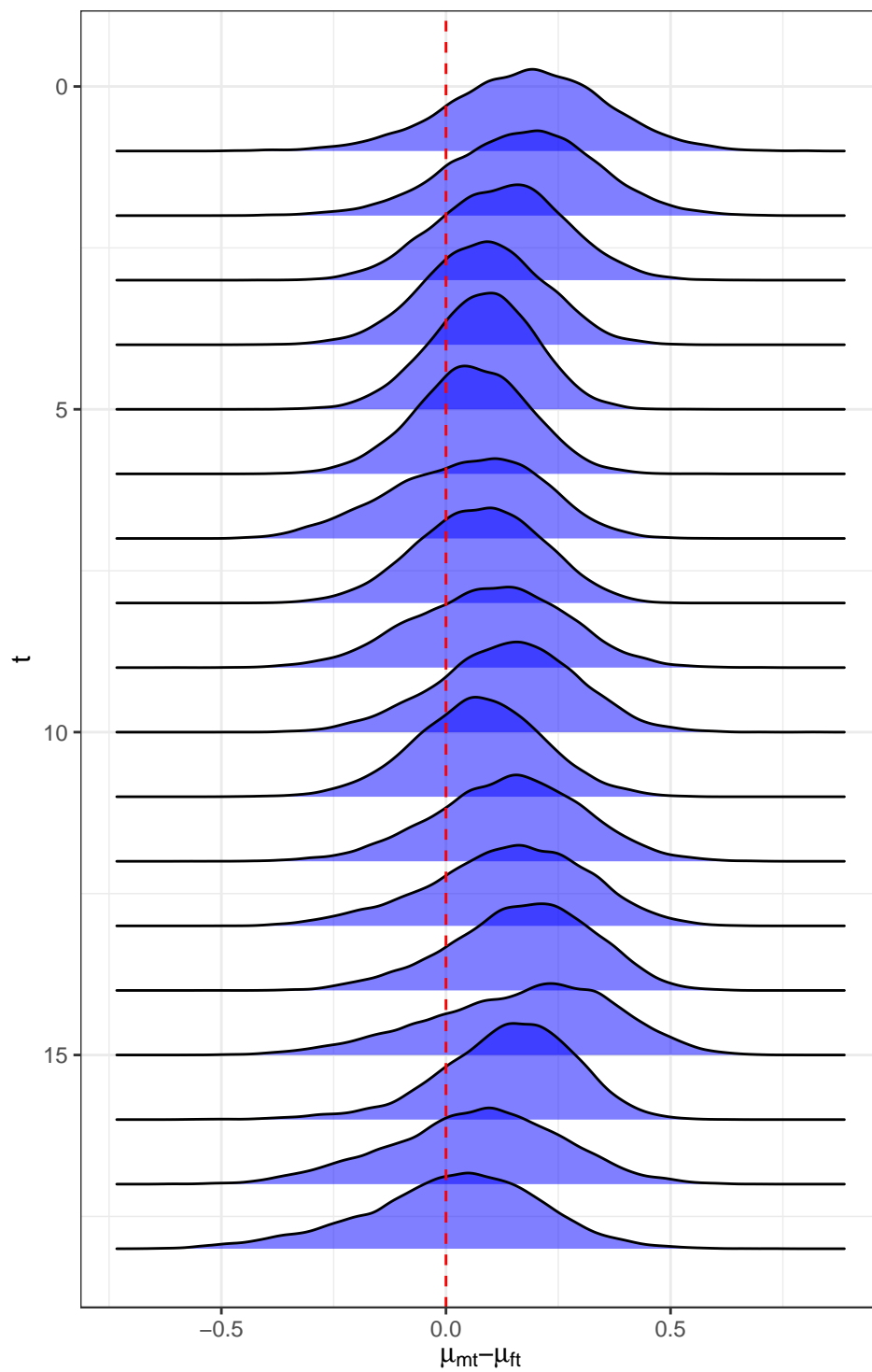


Figure 10: lpt

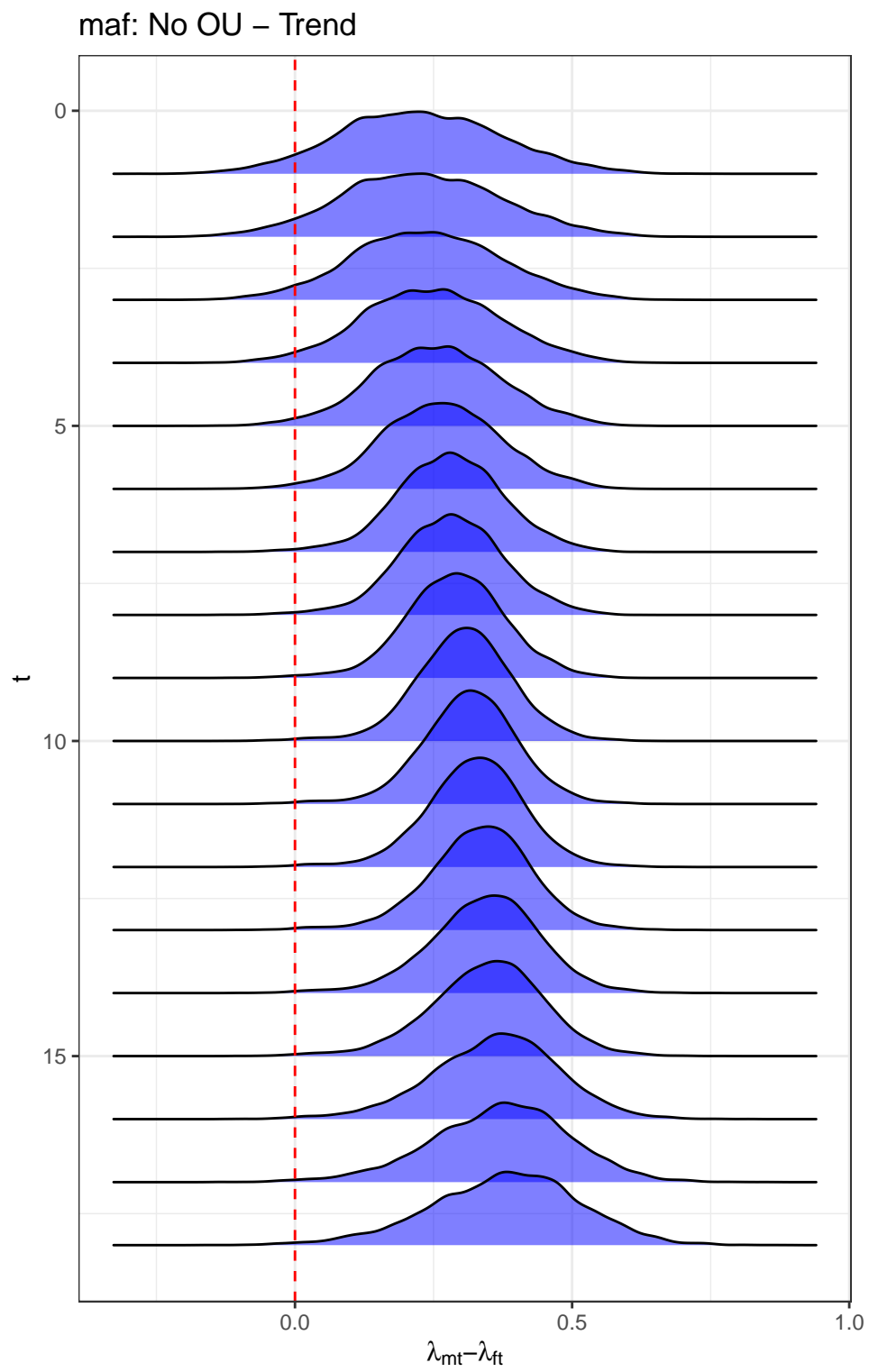


Figure 11: maf

mav: OU – No Trend

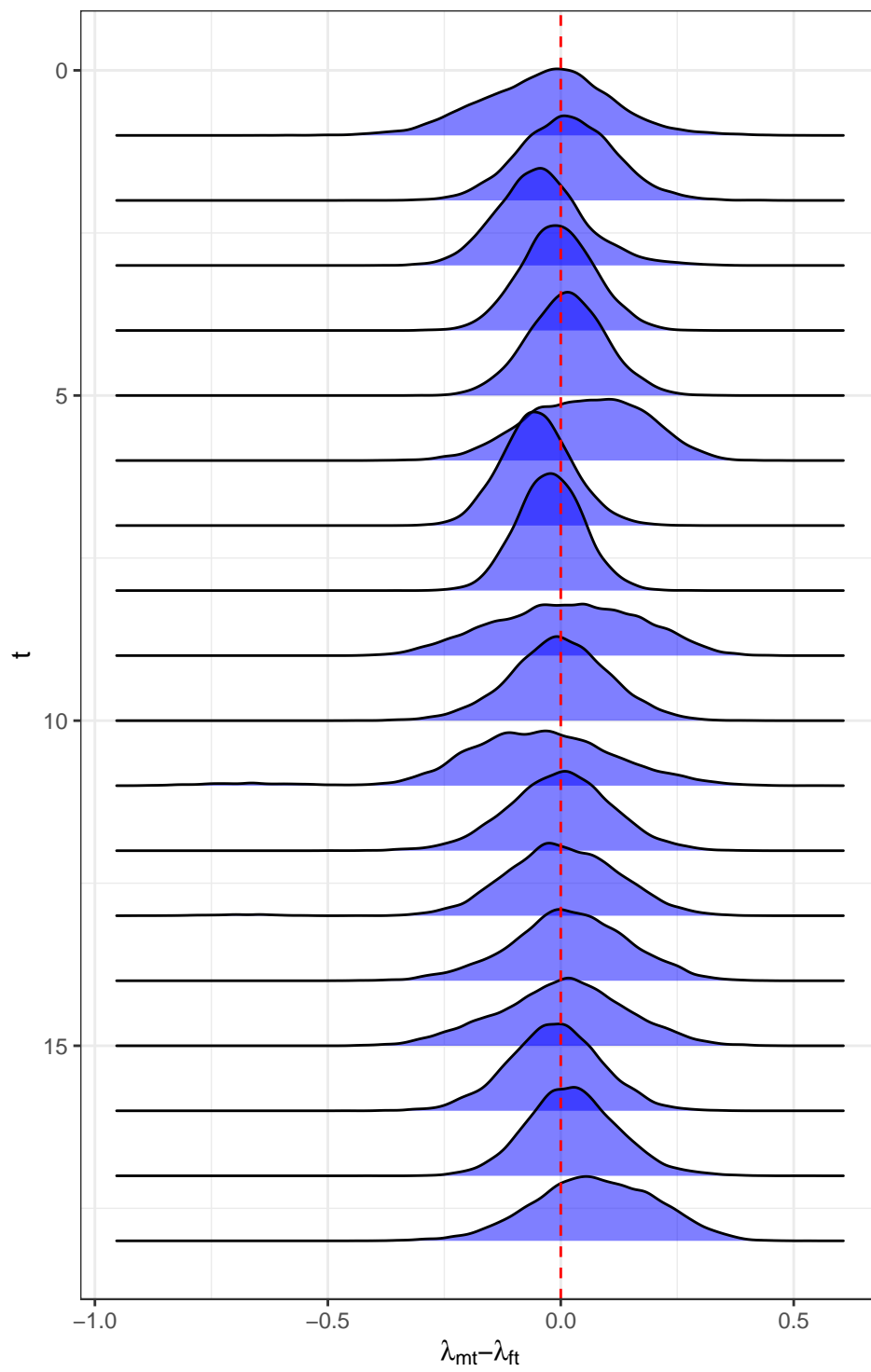


Figure 12: mav

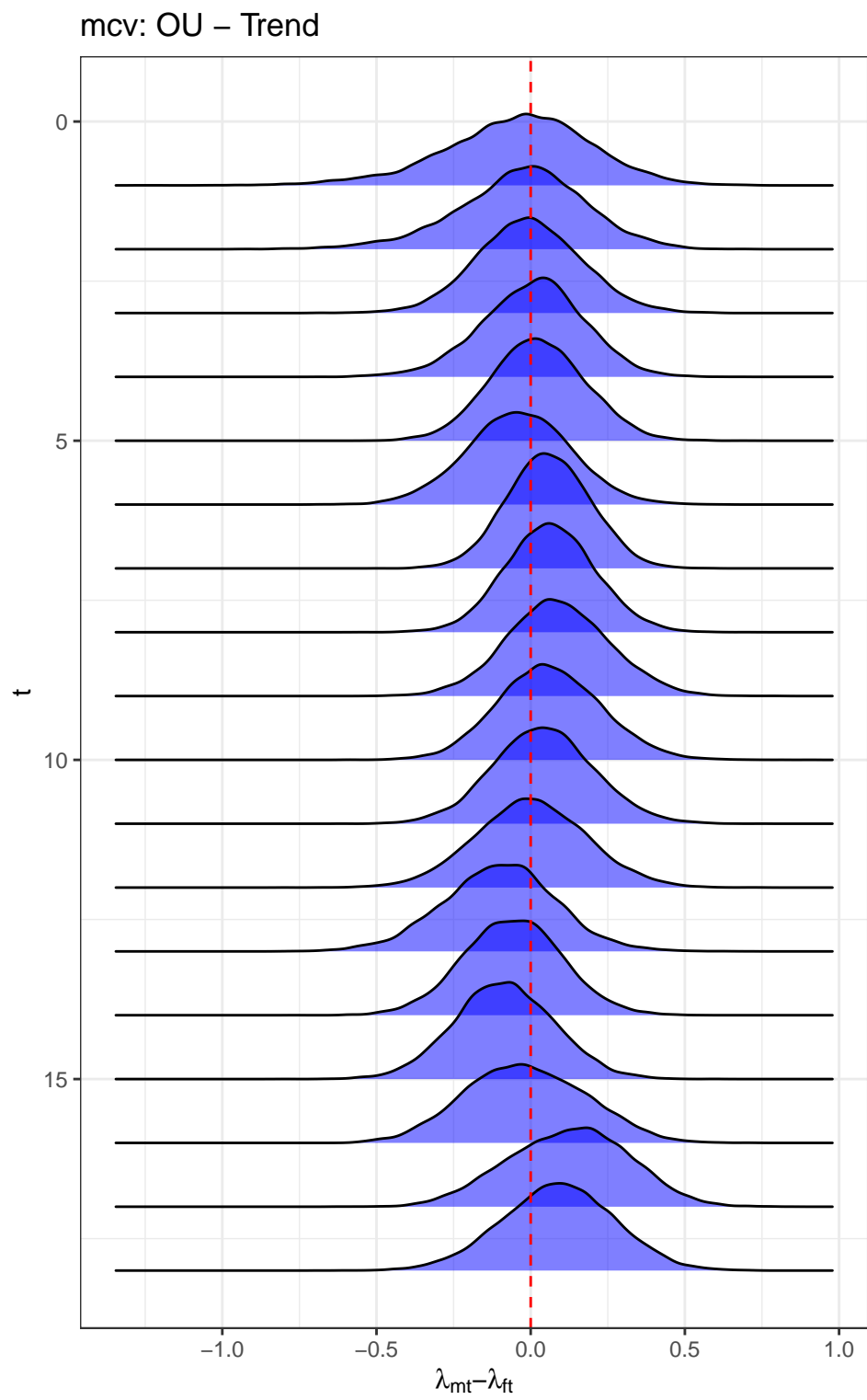


Figure 13: mcv

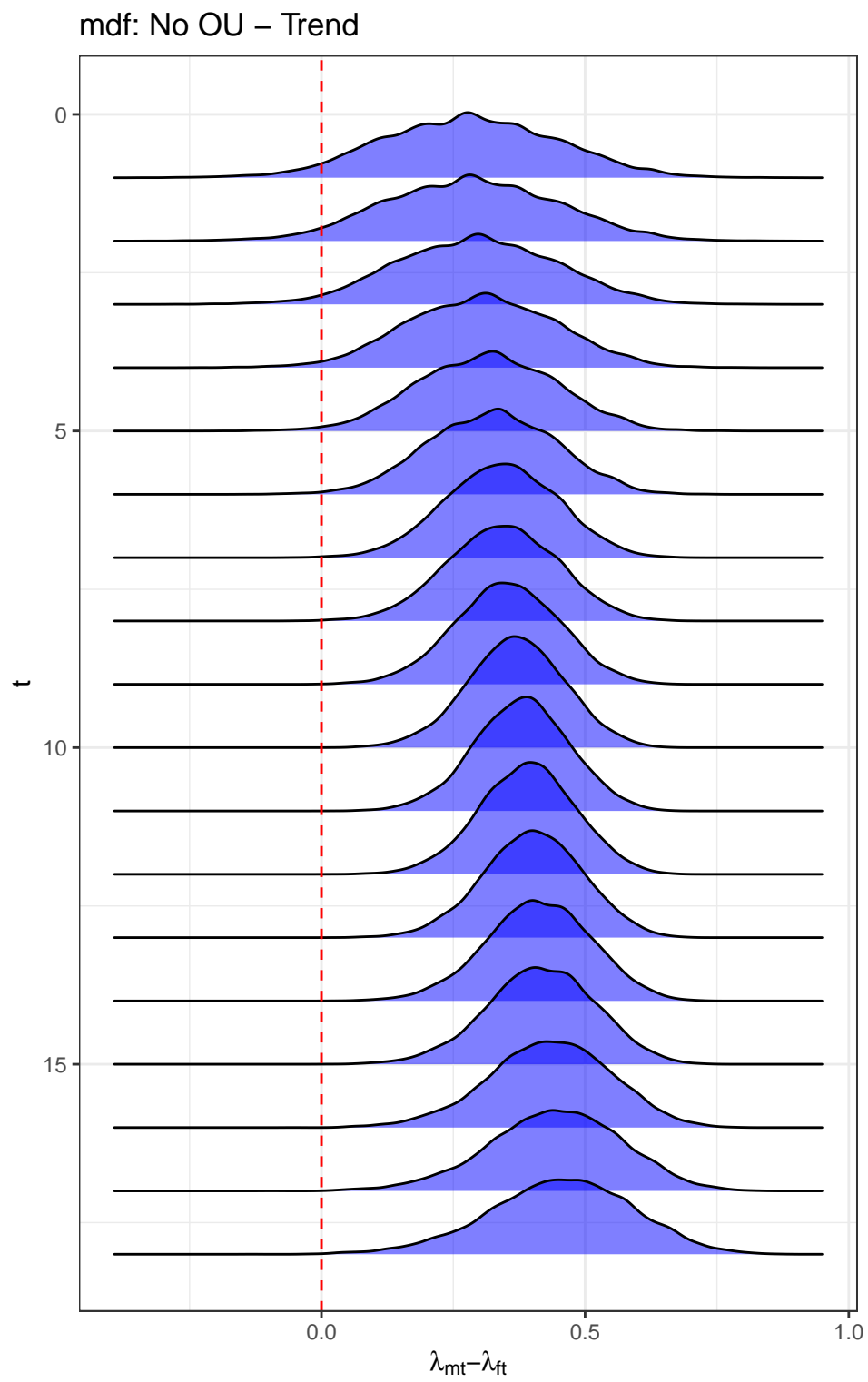


Figure 14: mdf

mds: No OU – No Trend

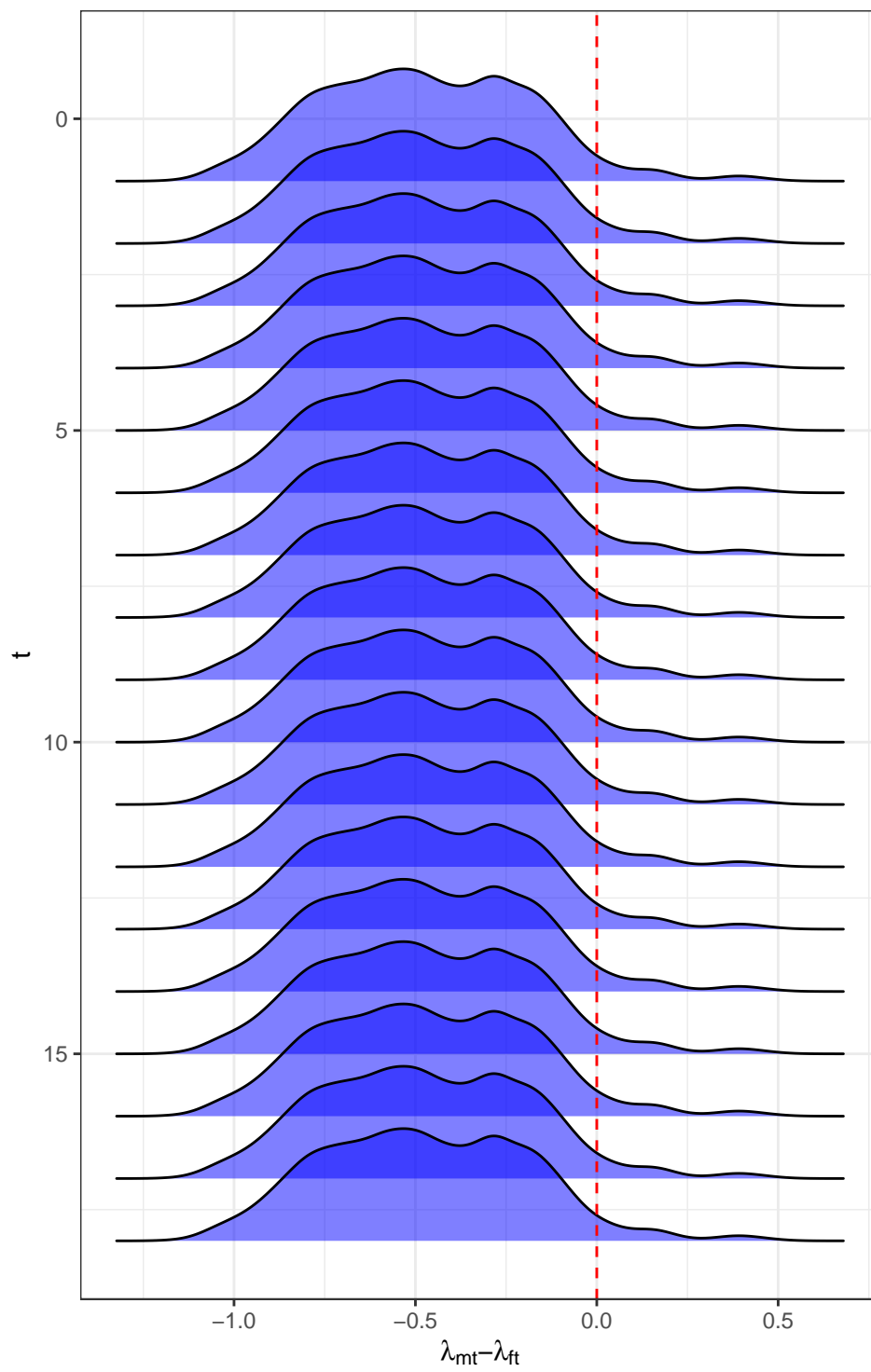


Figure 15: mds

mpt: No OU – No Trend

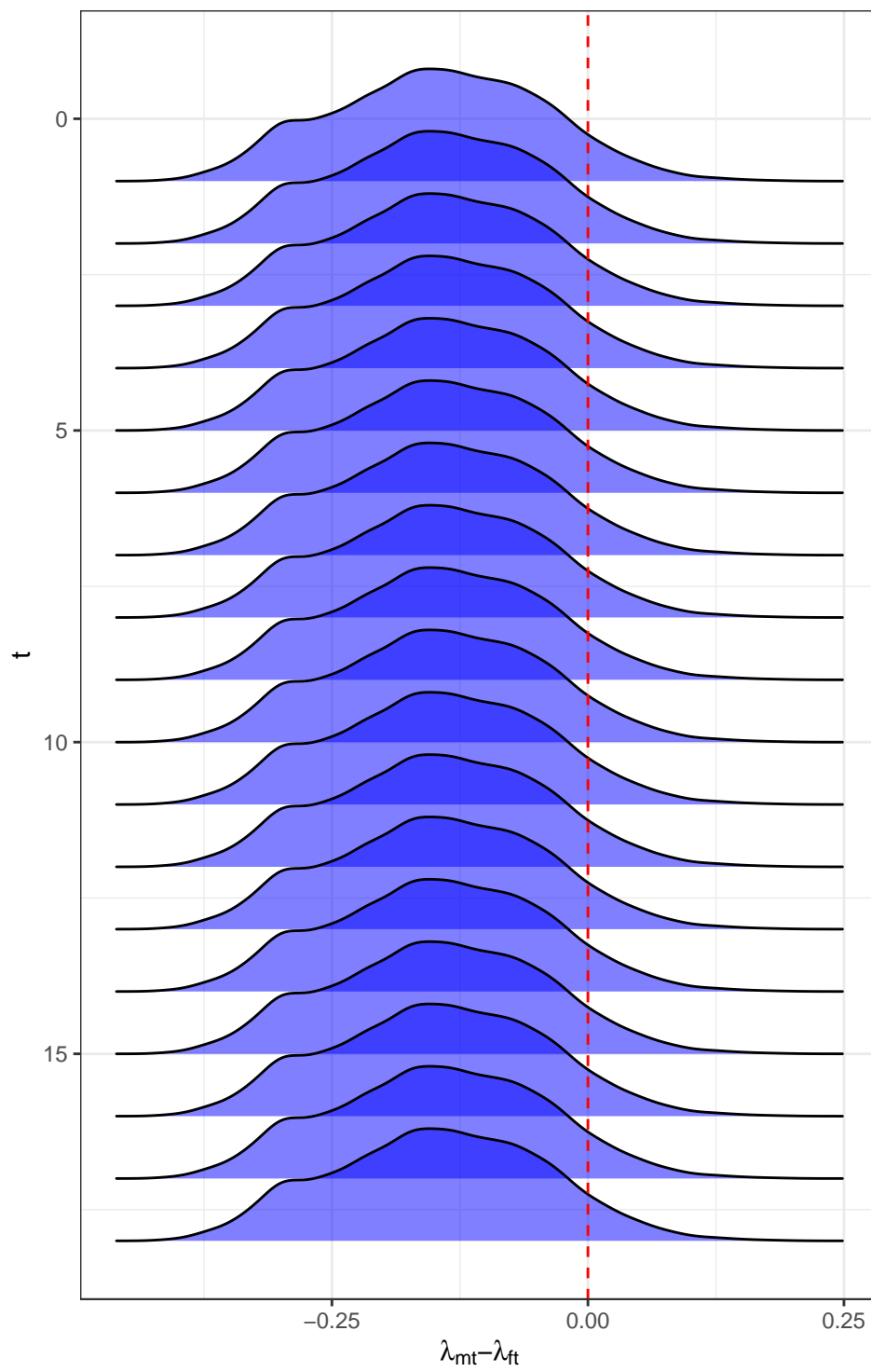


Figure 16: mpt

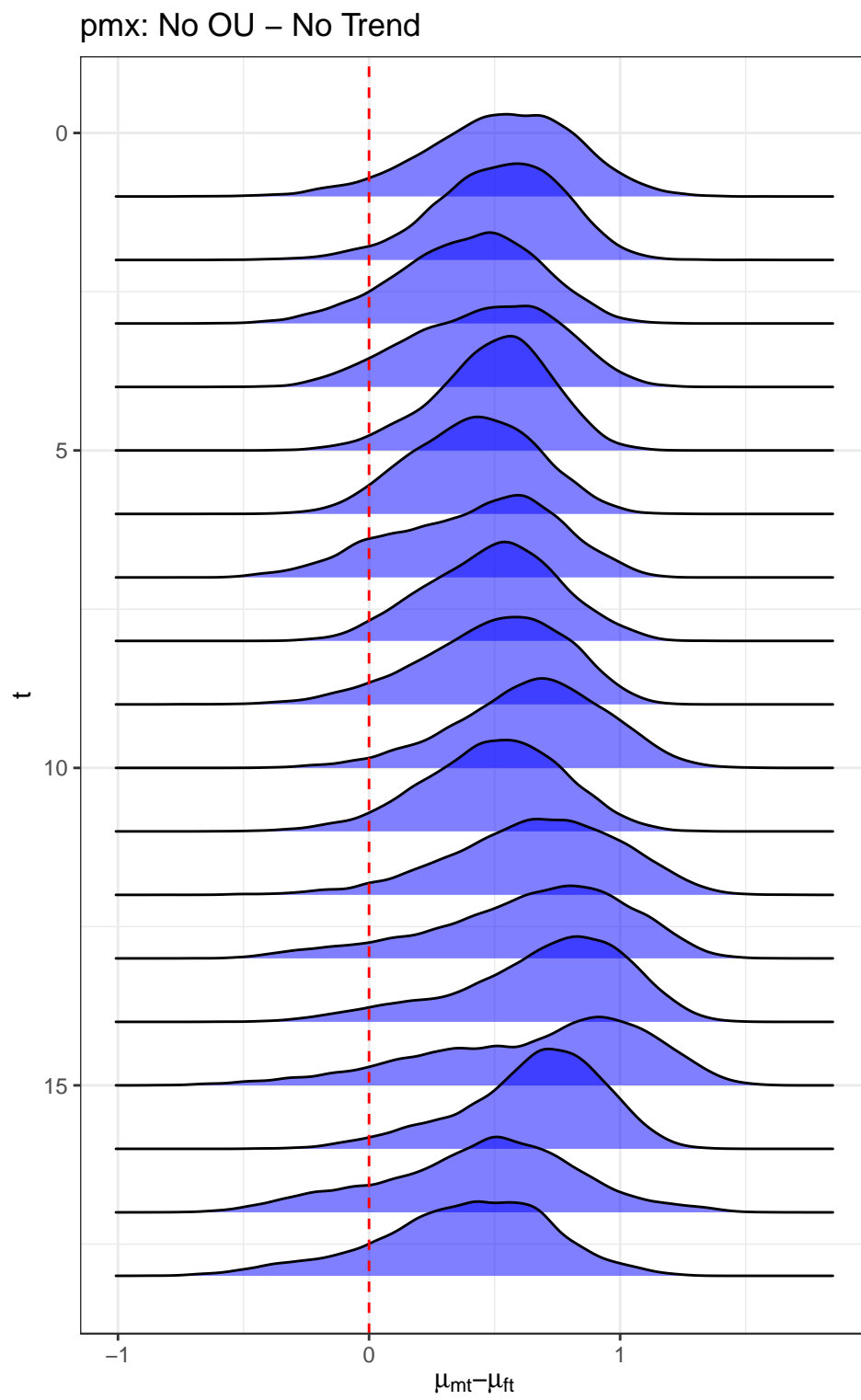


Figure 17: pmx

stl: OU – No Trend

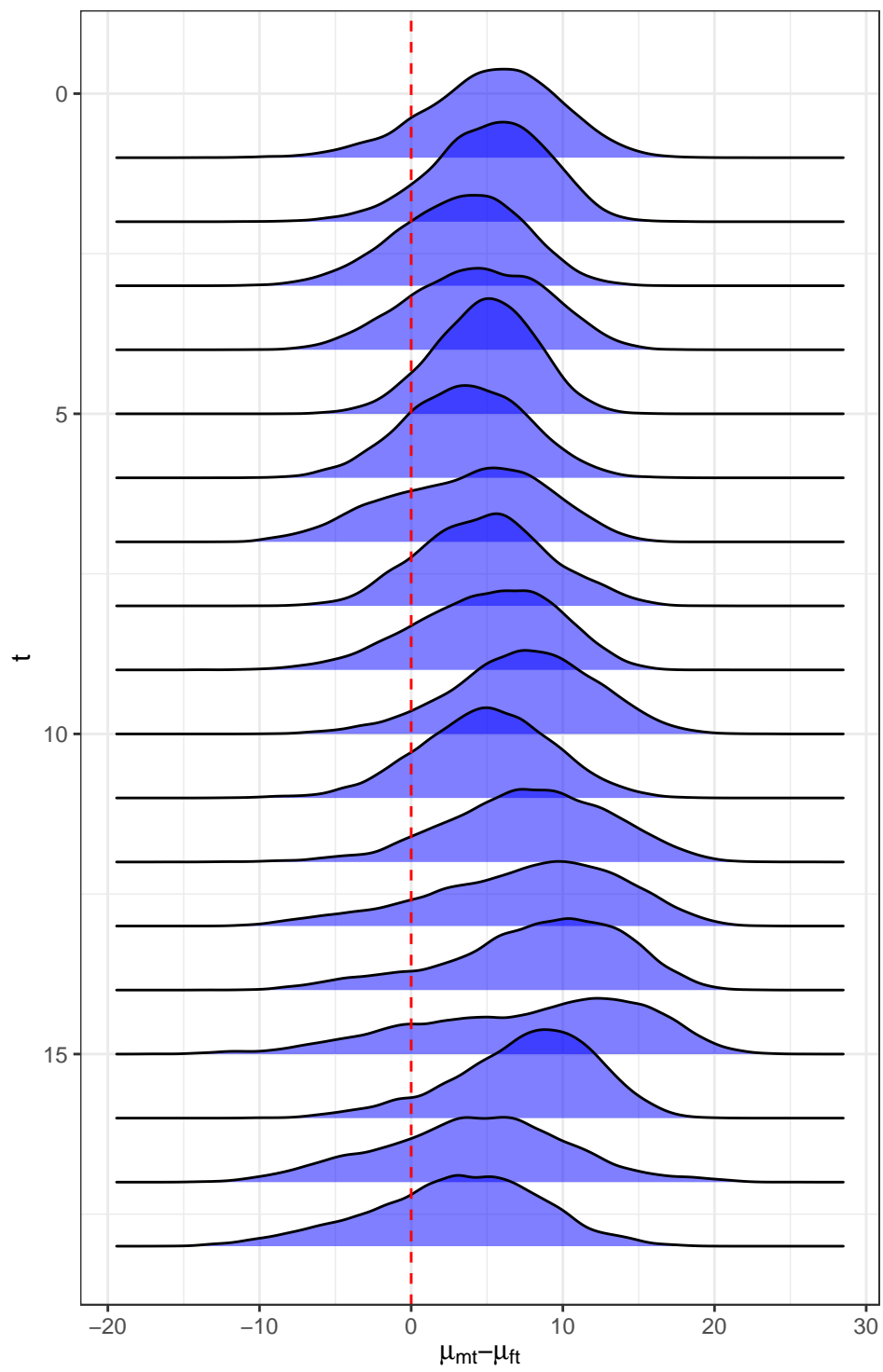


Figure 18: stl